Max-Planck-Institut
für Meteorologie

MAX-PLANCK-GESELLSCHAFT

International Max Planck Research School
on Earth System Modelling

West African Monsoon Rainfall in a Warming Climate

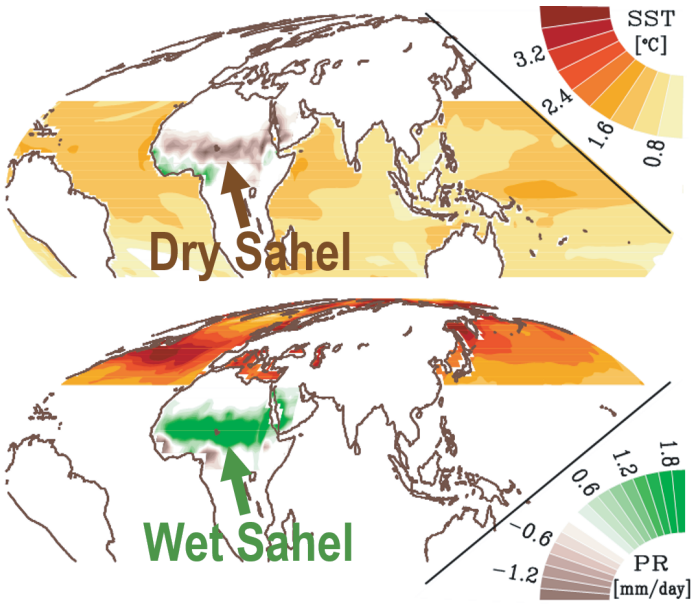

Jong-yeon Park

Hamburg 2015

Berichte zur Erdsystemforschung
Reports on Earth System Science

175
2015

Hinweis

Die Berichte zur Erdsystemforschung werden vom Max-Planck-Institut für Meteorologie in Hamburg in unregelmäßiger Abfolge herausgegeben.

Sie enthalten wissenschaftliche und technische Beiträge, inklusive Dissertationen.

Die Beiträge geben nicht notwendigerweise die Auffassung des Instituts wieder.

Die "Berichte zur Erdsystemforschung" führen die vorherigen Reihen "Reports" und "Examensarbeiten" weiter.

Notice

The Reports on Earth System Science are published by the Max Planck Institute for Meteorology in Hamburg. They appear in irregular intervals.

They contain scientific and technical contributions, including Ph. D. theses.

The Reports do not necessarily reflect the opinion of the Institute.

The "Reports on Earth System Science" continue the former "Reports" and "Examensarbeiten" of the Max Planck Institute.

Anschrift / Address

Max-Planck-Institut für Meteorologie
Bundesstrasse 53
20146 Hamburg
Deutschland

Tel./Phone: +49 (0)40 4 11 73 - 0
Fax: +49 (0)40 4 11 73 - 298

name.surname@mpimet.mpg.de
www.mpimet.mpg.de

Layout

Bettina Diallo and Norbert P. Noreiks
Communication

Copyright

West African Monsoon Rainfall in a Warming Climate

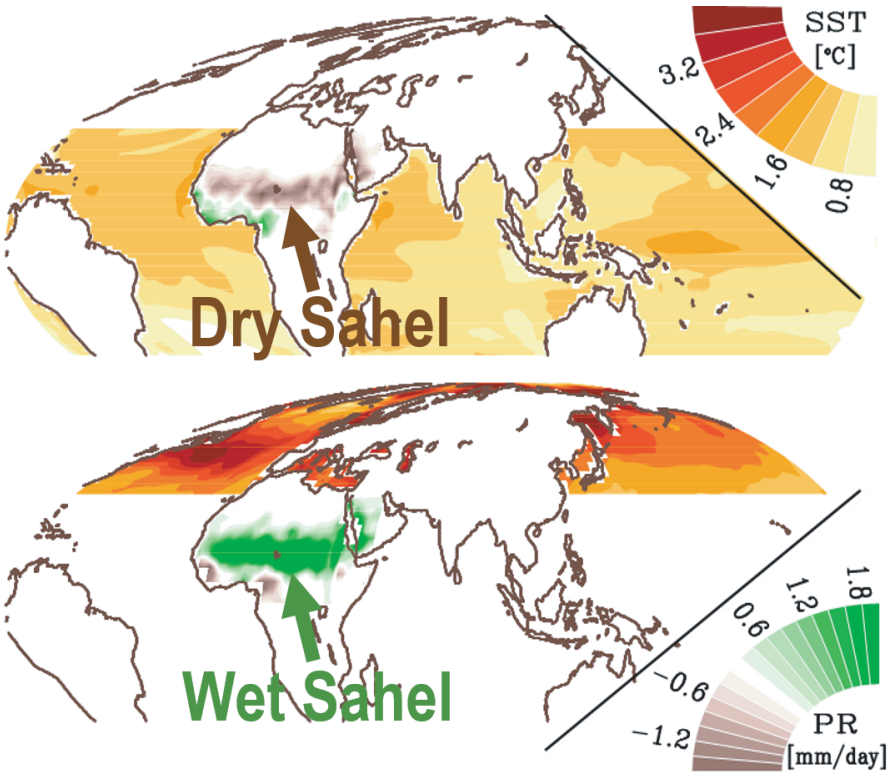

Jong-yeon Park

Hamburg 2015

Jong-yeon Park
aus Daegu, Südkorea

Max-Planck-Institut für Meteorologie
Bundesstrasse 53
20146 Hamburg

Als Dissertation angenommen
vom Fachbereich Geowissenschaften der Universität Hamburg

auf Grund der Gutachten von
Prof. Dr. Martin Claußen
und
Dr. Jürgen Bader

Hamburg, den 10. 12. 2015
Professor Dr. Christian Betzler
Leiter des Departments Geowissenschaften

Berichte zur Erdsystemforschung / Max-Planck-Institut für Meteorologie 175
Reports on Earth System Science / Max Planck Institute for Meteorology 2015

ISSN 1614-1199

Abstract

The Sahel, the semi-arid zone located along the southern margin of the Sahara and inextricably linked to the West African Monsoon, experienced one of the most remarkable decadal variability of monsoon rainfall. Given the historical climate-related calamities in this vulnerable area, a reliable prediction of future Sahel rainfall is essential to adapt to future climate changes. However, future Sahel rainfall projections from climate models are highly uncertain, showing even the opposite sign of the trends. Moreover, the 20th century cross-model consensus linking Sahel rainfall to tropical sea-surface temperatures (SSTs) breaks down for the 21st century. This thesis shows that the diverse future Northern Hemisphere (NH) differential warming between extratropical and tropical SSTs is the source of the future Sahel rainfall discrepancy. The SST-Sahel rainfall linkage that holds for the 20th century persists into the 21st century when this certain differential SST warming is taken into account. A suite of SST-sensitivity experiments confirms that strong NH extratropical warming substantially increases Sahel rainfall, which can predominate over the drying impact of tropical SST warming.

A further analysis reveals that the Mediterranean Sea is the key area in the pathway of the NH extratropical warming impact on Sahel rainfall. The wetting impact of Mediterranean Sea warming can become dominant in a warming climate, overweighing impacts of other extratropical ocean basins. This emerging role of the Mediterranean Sea is also seen in the recent period. The observed recovery of Sahel rainfall is found to be largely driven by anthropogenic Mediterranean warming. This is distinguished from past Sahel rainfall variations dominated by tropical SSTs. The dominant impact of Mediterranean warming on present and future Sahel rainfall provides an insight into the mechanism how the NH extratropical warming increases Sahel rainfall. Contrary to common belief, the northward shift of tropical rain belt by an interhemispheric thermal gradient is not the main cause of the Sahel rainfall increase under the strong NH extratropical warming. Rather, a local ventilation effect by the enhanced low-level moisture inflow from the warmer northern ocean plays a more important role.

Contents

List of Abbreviations and Acronyms

WAM - West African Monsoon

(The terms 'West African Monsoon rainfall' and 'Sahel rainfall' are used interchangeably)

JAS - July-August-September

SST - Sea Surface Temperature

NH - Northern Hemisphere

SH - Southern Hemisphere

AGCM – Atmospheric General Circulation Model

CMIP - Coupled Model Intercomparison Project

AMIP - Atmospheric Model Intercomparison Project

ITCZ - Inter Tropical Convergence Zone

Overview

The West African Monsoon is characterized by the seasonal migration of the tropical rain belt and the peak rainy season from July to September. The West African Monsoon rainfall exhibits strong low-frequency variability which has caused devastating environmental and socio-economic impacts. Intensive studies on the historical monsoon rainfall variations have shown that the past decadal variability is mainly caused by a certain distribution of SSTs in observations and models alike.

In contrast to the relatively well understood historical evolution, the future development of the West African Monsoon rainfall is known for its mysterious behaviour in the 21st century projection. The cross-model consensus in simulating historical rainfall does not guarantee consistent and reliable future predictions. Several studies suggested that future Sahel rainfall cannot be explained by the previously-known Sahel rainfall-SST linkage, but might be controlled by other factors such as direct radiative forcing, land surface processes, or atmospheric circulation changes.

The aim of this thesis is to understand the disagreement in projected Sahel rainfall trends. In Chapter 2, a main source of the model discrepancy is suggested. Statistical analyses with multi-model outputs and a suite of SST-sensitivity experiment show that the competing influence of the extratropical and tropical oceanic warming is the key to understanding the future Sahel rainfall uncertainty. If a model projects a NH differential warming involving the stronger extratropical warming compared to tropical warming, the wetting impact of extratropical warming can overweigh the drying impact of tropical warming, and consequently leading to a wet condition in the future Sahel and vice versa.

Chapter 3 comprises the mechanism how the NH differential warming determines future Sahel rainfall. By examining the individual impact of tropical and extratropical

warming on the West African Monsoon rainfall, a mechanistic understanding of future Sahel rainfall change is obtained. Particularly, the warming in the Mediterranean See is found to be a key SST area in the relationship between the NH extratropical warming and Sahel rainfall increase.

In Chapter 4, the dominant impact of future Mediterranean Sea warming is further investigated. The wetting impact of Mediterranean Sea warming on Sahel rainfall linearly increases with the magnitude of SST warming, whereas warming in other NH extratropical ocean basins does not show such a distinct increase of the wetting impact. This leads to a more important role of the Mediterranean warming in the future than in the past. The similar result is also obtained in the recent observed period.

The dominant impact of Mediterranean warming compared to the impacts of warming in other NH extratropical ocean basins may provide a new insight into understanding how the Sahel rainfall will change in the future. Given that most climate models project a stronger warming in the NH extratropics than the tropics, it is often assume that the northward shift of tropical rain belt to balance the atmospheric energy transport is the main mechanism of the Sahel rainfall increase. In Chapter 5, to tackle the common assumption, the relative contribution of the global-scale Inter Tropical Convergence Zone (ITCZ) shift effect and local monsoon process is examined by performing a suite of aqua-planet experiments with an idealized land.

Finally, the last chapter describes a summary of this study and some possible future work that still need to be advanced and would be carried out after this study.

This thesis is based on three papers which are listed below.

- Park, J.-Y., J. Bader, and D. Matei, 2015: Northern-hemispheric differential warming is the key to understanding the discrepancies in the projected Sahel rainfall. *Nature Communications*, **5,** 1-8. ·····Chapter 2, 3
- Park, J.-Y., J. Bader, and D. Matei, 2015: Anthropogenic Mediterranean warming essential driver for present and future Sahel rainfall. *Nature Climate Change, under review*. ·····Chapter 3, 4
- Park, J.-Y., J. Bader, and D. Matei, 2016: Local monsoon process vs. global-scale ITCZ shift: Which impact is more dominant for regional climate changes in a semi-arid tropical continent? *In preparation.* ·····Chapter 5

1 Introduction

The African Sahel region has experienced one of the most pronounced decadal fluctuations in rainfall. Due to the vulnerability of socio-economic as well as climate systems in the Sahel region, understanding the historical and future Sahel rainfall has been of great interest in climate science over the past decade. This chapter provides an overview of the current knowledge on the historical Sahel rainfall and introduces an unresolved scientific question about future rainfall projections.

1.1 The Sahel zone of West Africa

The Sahel is a band of semi-arid region, covering parts of Senegal, Mauritania, Mali, Niger, Chad, and Sudan (Figure 1.1). Most of the countries in this region are the poorest countries in the world and the least developed at the global level. People are constantly suffering from food insecurity, political instability, epidemics, and violent conflicts. Even in recent years, an estimated 20 million people remain food insecure at the beginning of 2015 and more than 10% of those people have already crossed the crisis threshold (CARE 2015). Moreover, 5 million children younger than 5 are at risk of malnutrition. All these socio-economic vulnerabilities cause the Sahel region in a state of chronic threats of food insecurity.

Figure 1.1. The Sahel region across Africa from Senegal in the west to Sudan in the East (from 'https://libraryeuroparl.files.wordpress.com/2014/03/sahel_map2.jpg').

Besides the socio-economic vulnerability, the climate system in the Sahel region is also highly vulnerable to regional and remotely-forced climate variability. The Sahel region has experienced the strongest drying trend in the world during the twenty century (Figure 1.2). It also shows one of the most pronounced decadal variability exhibiting anomalously strong rainfall in the 1950s and early 1960s, followed by a devastating dry period since the 1970s (Figure 1.3) (Folland et al. 1986; Nicholson 2005; Kaptué et al. 2015). This climatic vulnerability generally makes the society even more vulnerable due to the agricultural society living primarily from crops and livestock.

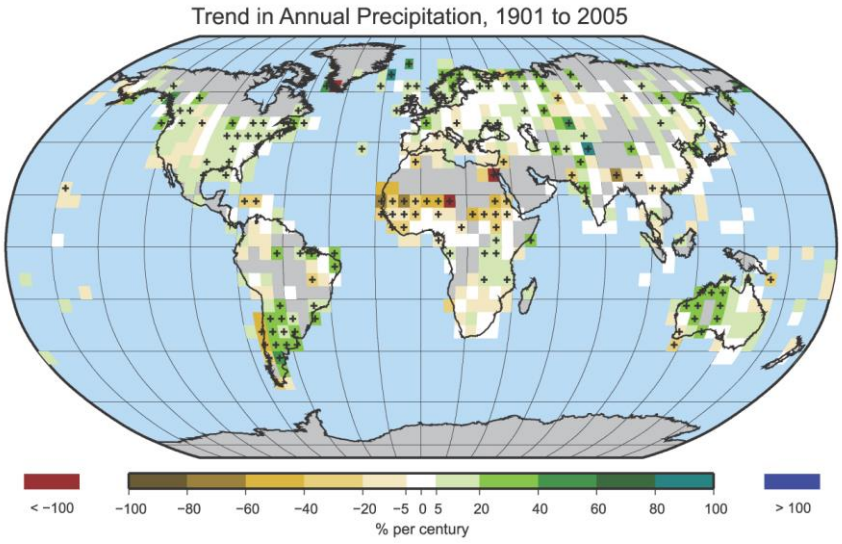

Figure 1.2. Trend of annual land precipitation for 1901 to 2005 (% per century) from IPCC report (Fig.3.13 in IPCC 2007). The percentage is based on the means for the 1961 to 1990 period. Areas in grey have insufficient data to produce reliable trends. Trends significant at the 5% level are indicated by black marks.

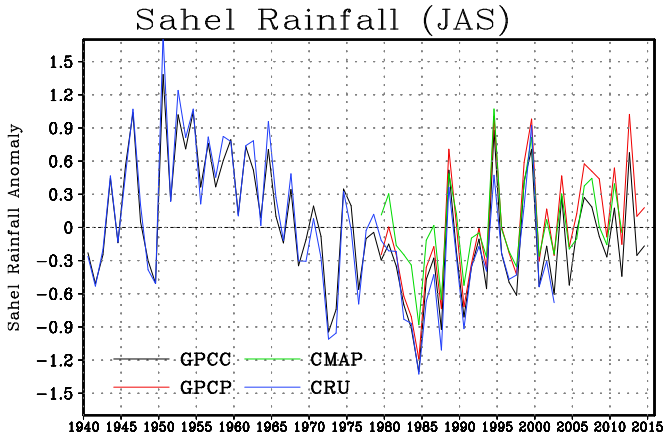

Figure 1.3. Time series of observed summer (July-August-September) mean rainfall anomalies (unit: mm day^{-1}) over the Sahel (10°W-30°E; 10°-20°N) derived from 4 different precipitation datasets, GPCC, CMAP, GPCP, and CRU.

Statistics on the impact of the past Sahel drought supports the climate-driven vulnerability of this society. During the persistent drought period in the 1970/1980s, most of the Sahel's 50 million people suffered from water and food insecurity including 100,000 of death and 750,000 of people who urgently of food-aid-dependency (AMCEN 2002). In addition, the drought resulted in a substantial loss in crop yield with soaring food prices. According to the United Nations, up to 250 million people in Africa are projected to suffer from water scarcity within this century and three-quarters of cropping land in the Sahel will be substantially affected by climate change (United_Nations 2015).

1.2 Historical West African Monsoon (WAM) rainfall

The summer rainfall over the semiarid African Sahel is known for its pronounced multi-decadal variability over the past century as shown in Figure 1.3. Particularly, the persistent Sahel drought in the 1980s is the strongest inter-decadal climate signals among all recent observational records in global monsoon regions (Ward 1998; Trenberth et al. 2007). Since the devastating drought period during which millions of West Africans died of hunger-related causes and development was hampered, a general consensus has been established that understanding Sahel rainfall variations is fundamental for this vulnerable society to prepare for future changes in water

availability. The following subsections introduce the general features of WAM and the key factors controlling the historical monsoon rainfall.

1.2.1 Characteristics of West African Monsoon

The main characteristics of the WAM are the strong seasonal wind reversal and the north-south migration of tropical rain belt, which are similar features to other monsoon systems (Ramage 1971). The north-easterly wind, known as the 'Harmattan', is prevailing in boreal winter over the Sahel region, while the south-westerly wind is dominant in summer (Figure 1.4). The monsoon rainfall is linked to the moisture confluence between the northerly and southerly monsoonal winds, which is of prime importance for the WAM system by providing moisture to the ascent column. Thus, the latitudinal location of tropical rain band appears to be coherent with the seasonal wind change. The rain band migrates northward from the equatorial Atlantic in winter, reaches the Sahel region in summer, and then moves back to the south in the following winter.

The seasonal march of tropical rain band is better represented in the zonal mean precipitation plot (Figure 1.5). The rain band starts to affect the Sahel region since late spring and leads to a maximum monsoon rainfall in July to September. One distinctive feature of WAM rainfall is the abrupt latitudinal shift of maximum precipitation from the Guinean coast in June into the Sahel region in August, which is known as the West African Monsoon jump.

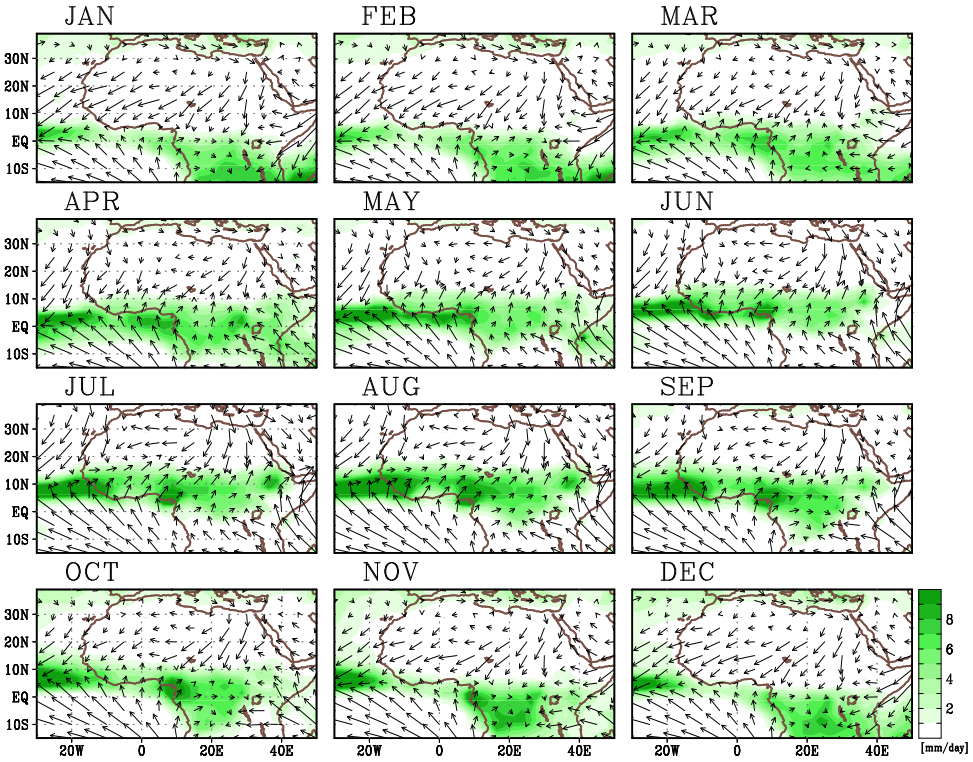

Figure 1.4. The climatological monthly-mean rainfall (shading, unit: mm day^{-1}) and 925 hPa wind (arrows, unit: m s^{-1}) during the period 1979-2010. The precipitation data is obtained from the CMAP, and the wind data is from the NCEP2 reanalysis.

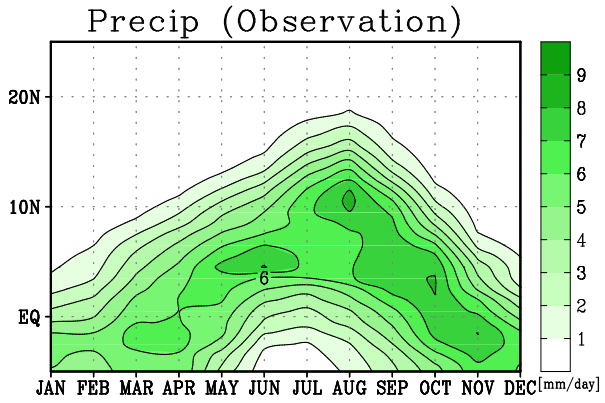

Figure 1.5. Longitudinal mean (10°W-30°E) of GPCC precipitation (unit: mm day^{-1}) over the African continent.

1.2.2 Factors controlling low-frequency variability of monsoon rainfall

Intensive studies on the historical Sahel rainfall have shown that oceanic forcing is the dominant driver of the observed low-frequency variability of Sahel rainfall (Fontaine et al. 1998; Ward 1998; Bader and Latif 2003; Giannini et al. 2003; Rowell

2003; Lu and Delworth 2005; Hoerling et al. 2006). An AGCM forced by historical SSTs can reproduce well the historical low-frequency variability of Sahel rainfall (Figure 1.6a). Land surface processes and vegetation feedbacks which can amplify the SST-driven rainfall anomalies (Zeng et al. 1999) and the upper jets which can enhance the ascent over the Sahel (Nicholson 2008, 2009a) are also known as additional factors modifying the intensity of monsoon rainfall. The underlying SST changes associated with the historical Sahel fluctuation include anomalies mainly in the Atlantic (Hastenrath 1990; Vizy and Cook 2001) and Indo-Pacific (Janicot et al. 1996; Bader and Latif 2003) as shown in Figure 1.6b. For example, a positive north-south gradient of the tropical Atlantic SST anomalies [(70°-20°W, 5°-30°N) minus (40°W-5°E, 30°S-5°N)] shifts the Atlantic ITCZ northward and provides more moisture to the Sahel. The cooling in the Indian Ocean and tropical Pacific (50°E-90°W, 20°S-20°N) reduces the atmospheric stability in the tropical troposphere and constitutes a favourable condition for the enhanced convection over the Sahel, and vice versa. Mediterranean SST anomalies are also acknowledged to partly contribute to the drought period (Rowell 2003; Gaetani et al. 2010). An interhemispheric asymmetry of global SST anomalies which may include some of aforementioned regional SST anomalies has been also recognized as an important component of the Sahel rainfall change by meridionally shifting the tropical rainbelt (Folland et al. 1986; Chiang and Friedman 2012). Additional forcing from aerosols and greenhouse gases may contribute to the rainfall change by directly influencing local land surface process and indirectly affecting via global SST anomalies (Rotstayn and Lohmann 2002; Booth et al. 2012).

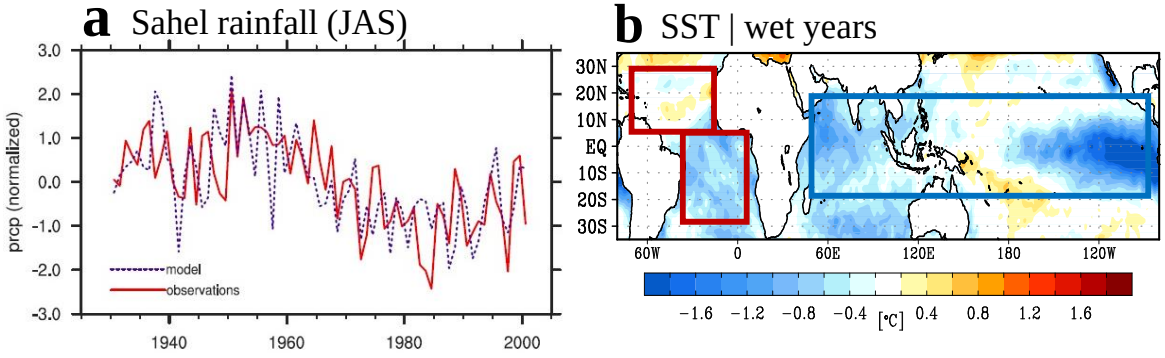

*Figure 1.6. **a**. Observed (red) and modelled (blue) JAS (July-September)-mean Sahel rainfall from Giannini et al. 2003. An AGCM is forced with historical SSTs in their simulations, but*

keeping all other forcing constant in time. ***b****, Composite difference of JAS-mean SSTs between the wet and dry years in the Sahel region during the period 1940-2013. Red and blue boxes represent the key SST areas that dominate historical Sahel rainfall variations.*

1.3 Future West African Monsoon rainfall

Understanding and predictability of future WAM rainfall are important for this vulnerable society to prepare for and adapt to future changes in water availability. The following subsections present how climate models project future Sahel rainfall and how discrepant the rainfall projection is.

1.3.1 Uncertainty in future Sahel rainfall projections

The rainfall over the African Sahel region is known for its puzzling behaviour in the 21st century projections (Cook and Vizy 2006; Douville et al. 2006; Joly et al. 2007; Biasutti et al. 2008; Cook 2008; Caminade and Terray 2010). Future Sahel rainfall projections in different climate models are disagreeing even on the sign of the trend (Figure 1.7). Given the robust drying in response to late 20th century forcing factors of the same coupled models (Biasutti and Giannini 2006), such disagreement for future Sahel rainfall is surprising.

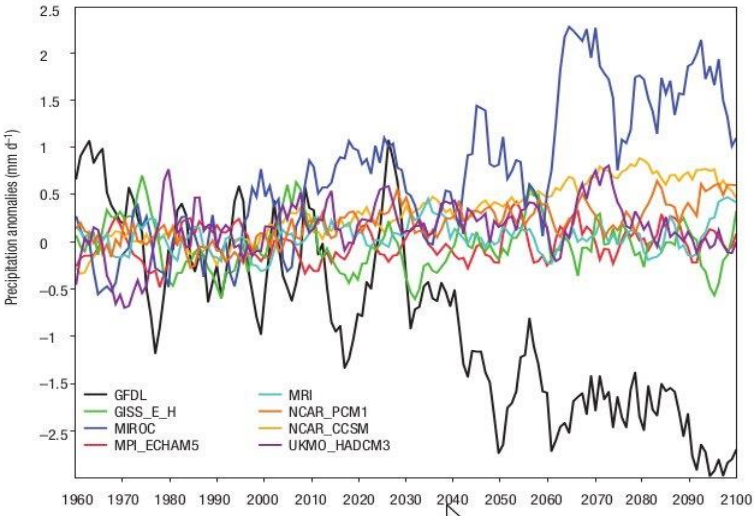

Figure 1.7: The JAS-mean Sahel rainfall anomalies from CMIP3 models. This figure is from Cook 2008 ('News & Views' in Nature).

The uncertainty regarding the future rainfall found in the previous generation of climate models, i.e. the Coupled Model Intercomparison Project (CMIP3) models, still exists even in the new generation of climate models, i.e., CMIP5 (Figure 1.8). For example, as shown in the future projection from GFDL and MIROC models in CMIP3 (Biasutti et al. 2008; Cook 2008), two CMIP5 models from the same family, GFDL-ESM2M and MIROC-ESM, still project a substantially dryer and wetter Sahel, respectively, under a medium future emission scenario (Representative Concentration Pathways 4.5; RCP4.5). A recent study using the strongest radiatively forced future scenario for CMIP5 also supports the diversity of future Sahel rainfall trends (Biasutti 2013). Those two extreme simulations cannot be ignored because either the drying or wetting of the Sahel is a physically plausible response to increased radiative forcing, and these two models provide relatively accurate simulations of the West African summer rainfall in the historical period (Cook and Vizy 2006).

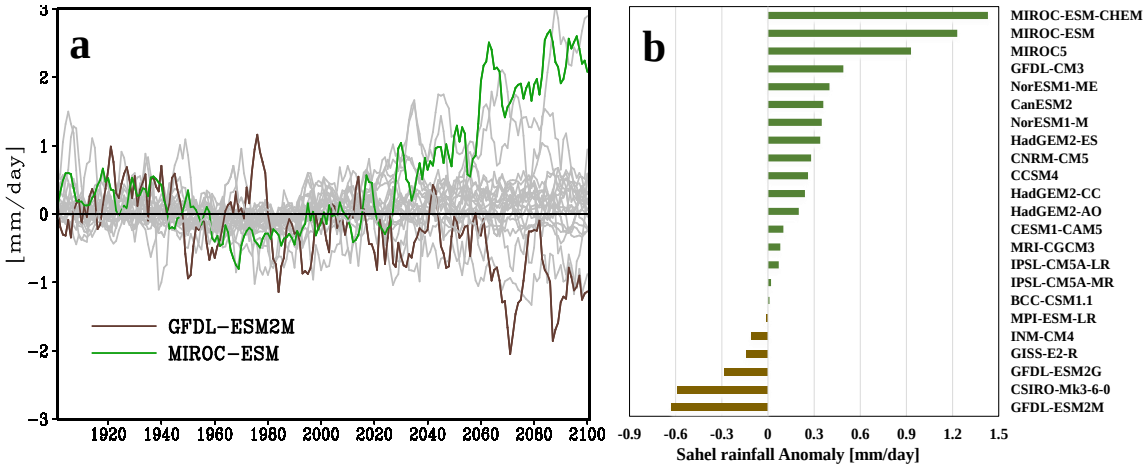

Figure 1.8. ***a,*** *Same as Figure 1.7 but for CMIP5 models.* ***b****, The future (2070-2099) JAS-mean Sahel rainfall anomalies from individual CMIP5 models. The anomalies are the differences from the mean of the historical run (1901-2005).*

1.3.2 Failure of future rainfall prediction by known SST-rainfall linkage

As addressed before, SST variations are recognised to be the main cause of the observed decadal Sahel rainfall variability (Bader and Latif 2003; Giannini et al. 2003; Haarsma et al. 2005; Held et al. 2005; Hoerling et al. 2006). Previous studies found that

the current models can capture the observed SST-Sahel rainfall relationship in both the pre-industrial and 20th century simulations. Thus, there has been an attempt to explain future Sahel rainfall based on its known historical relationship with tropical SSTs (Biasutti et al. 2008). Despite the dependence of Sahel rainfall on tropical SST anomalies in the past, however, the discrepancy in the future Sahel rainfall projection is not explained by different future SST anomalies in the tropics. Thus, it is often thought that SSTs may not be a source of the model discrepancy in the future Sahel rainfall.

One example of the inconsistent Sahel rainfall-SST relationship is shown in Figure 1.9. The Sahel rainfall simulated by MIROC-ESM, the fully-coupled model projecting a strong rainfall increase for the future Sahel, is linearly reconstructed using commonly-used tropical indices, which are the inter-hemispheric SST gradient index in the tropical Atlantic and the area-averaged Indo-Pacific SST index. Such a statistical model and indices are similar to the ones used in previous studies (Biasutti et al. 2008; Caminade and Terray 2010), which will be further explained in the next chapter. The two tropical indices reconstruct the Sahel rainfall reasonably well in the historical run, while they fail to reconstruct the future Sahel rainfall, exhibiting a drying trend in future Sahel rainfall. This confirms that the previously-used tropical SST indices are insufficient to predict a strong positive trend of future Sahel rainfall.

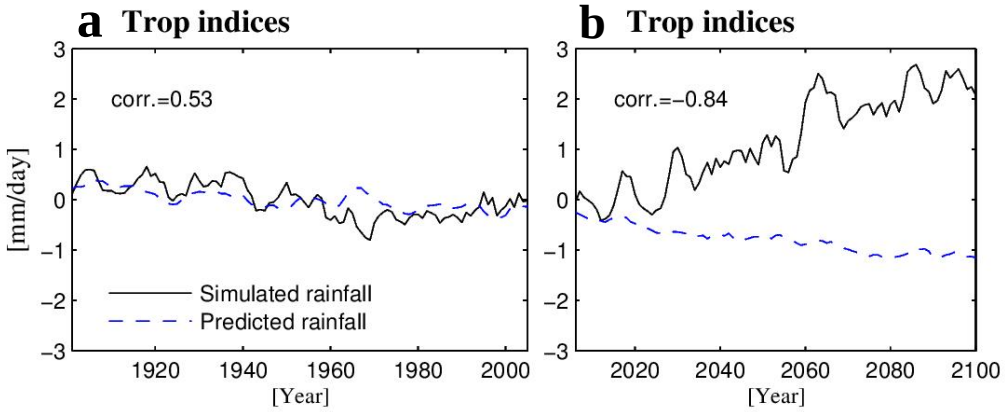

*Figure 1.9. Simulated Sahel rainfalls (black line) from a CMIP model, MIROC-ESM, and the linearly predicted Sahel rainfall (blue line) based on the two tropical SST indices (i.e. Atlantic SST gradient and Indo-Pacific SST) in the (**a**) historical and (**b**) future (RCP4.5) simulations. The coefficients of the multi-linear model are calculated from the historical simulation All indices are subjected to a five-year running mean.*

1.4 Research Objectives

After the failure of understanding the future Sahel rainfall development by using the historical SST-Sahel rainfall relationship, alternative explanations have been proposed regarding the source of the model discrepancy, such as the strength of the Sahara Low and the land surface response to radiative forcing (Biasutti et al. 2009; Giannini 2010). However, none of the previous studies has clearly found the cause of the model discrepancy and elucidated underlying mechanisms. Given that oceanic forcing has played the dominant role in shaping the observed variations of Sahel rainfall and previous studies mainly restricted their analysis to tropical SSTs, it is still necessary to extend the investigation to the role of global SSTs to understand the disagreement in projected Sahel rainfall trends. This raises scientific questions that I would like to answer in this thesis. The questions are as follows:

- What is the source of the model discrepancy in future Sahel rainfall projections?
- If an oceanic forcing still matters for the future Sahel rainfall, what kind of SST pattern in the global ocean is the most important?
- What is the underlying mechanisms of the future Sahel rainfall change?

2 NH differential warming: a key to understanding future Sahel rainfall

This chapter shows that **SSTs are still the fundamental factor in estimating future Sahel rainfall changes**. The difference between the historical period and future scenarios is that the key SST area determining Sahel rainfall changes will be shifted from the tropics to the Northern Hemisphere (NH) extratropics in the case of dominant future extratropical warming over tropical warming. A multi-model analysis reveals that future Sahel rainfall change can be substantially modified by the magnitude of extratropical warming, which is also confirmed by a series of SST-sensitivity experiments. A confident projection of future Sahel rainfall requires an understanding of the cause of the discrepancy in the rainfall projections by current climate models. The present work shown in this chapter contributes to such understanding by establishing NH differential warming as the crucial factor controlling the future Sahel rainfall uncertainty.[1]

[1] This chapter is mainly based on the following paper: Park, J.-Y., J. Bader, and D. Matei, 2015: Northern-hemispheric differential warming is the key to understanding the discrepancies in the projected Sahel rainfall. *Nature Communications*, **5,** 1-8

2.1 Multi-model analysis of future SST and Sahel rainfall

2.1.1 Data and method

2.1.1.1 CMIP5 archive

The multi-model data analysed here are obtained from the CMIP5 archive (Taylor et al. 2012). A total of twenty-three CMIP5 models, which provide SST and precipitation outputs during the period 1860-2100, are used in this study, focusing on the seasonal mean (July-August-September, JAS) values in which monsoon rainfall is most pronounced. In particular, much attention is devoted to analysing two models, 'GFDL-ESM2M' and 'MIROC-ESM', which project two opposite extreme anomalies of future Sahel rainfall. These two models originate from 'gfdl_cm2_1' and 'miroc3_2_medres' in CMIP3, which also predicted extreme drying and wetting, respectively. The two versions of models developed from the same modelling group are basically the same except for incorporating carbon dynamics and some minor tuning in physical models (Watanabe et al. 2011; Dunne et al. 2012). The future scenario chosen for the present study is the Representative Concentration Pathways 4.5 (RCP4.5), a mid-range mitigation scenario. All CMIP5 models used here are depicted in Figure 1.8b.

2.1.1.2 Statistical model to predict future Sahel rainfall

A statistical method is applied to see whether future Sahel rainfall can be explained by different future SSTs in models as shown in Figure 1.9. The statistical model used in our study is equivalent to the conventional multi-linear regression method, which is a standard technique to estimate the predictand from two or more explanatory variables. A best fit line is calculated by the least-squares method, minimising the sum of the squares of the deviations from the fitted line. The regression coefficients from the historical run is used for the future Sahel rainfall prediction. A cross-validation test, which is performed by calculating the coefficients from the future period and applying them to predict the historical rainfall, confirms the robustness of the statistical model.

2.1.2 Successful reproduction of future rainfall with extratropical warming

The uncertainty in future Sahel rainfall projection is largely caused by two models, GFDL-ESM2M and MIROC-ESM, that project an extreme dry condition and wet condition, respectively (Figure 1.7). In addition to the opposing Sahel rainfall projections, the two models also show a substantial difference in their projections of future Northern-hemispheric SST warming (Figure 2.1). In GFDL-ESM2M, the amplitudes of tropical and extratropical SST warming are similar, whereas in MIROC-ESM, extratropical warming is more prominent compared to the warming in the tropics, especially in the northern hemisphere (NH). Similar to a distinct difference in the amplitude of NH extratropical warming between GFDL-ESM and MIROC-ESM, other CMIP5 models projecting significant future drying and wetting Sahel confirm such distinct extratropical SST warming relative to the tropical warming (Figure 2.2). Therefore, it is worthwhile to investigate the role of NH extratropical SST warming in forcing the contradicting projections of future Sahel rainfall.

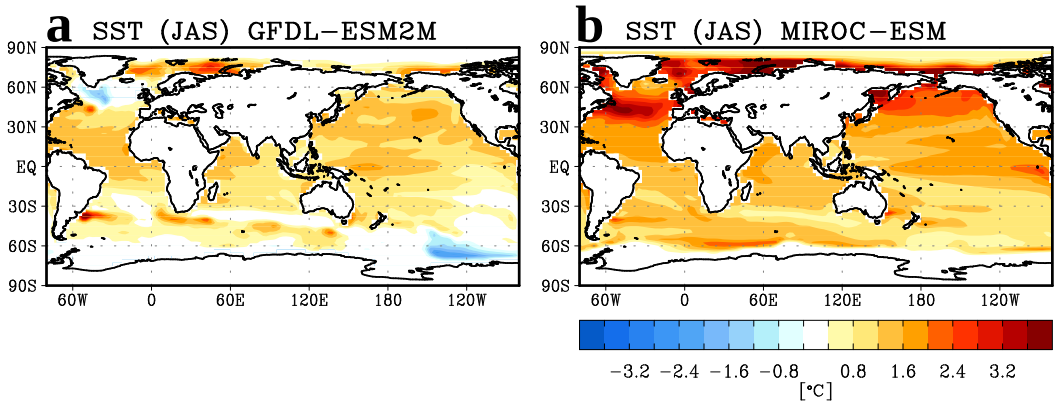

*Figure 2.1. SST differences between the 21st century and 20th century simulations from (**a**) GFDL-ESM2M and (**b**) MIROC-ESM, which project an extreme Sahel drying and wetting, respectively.*

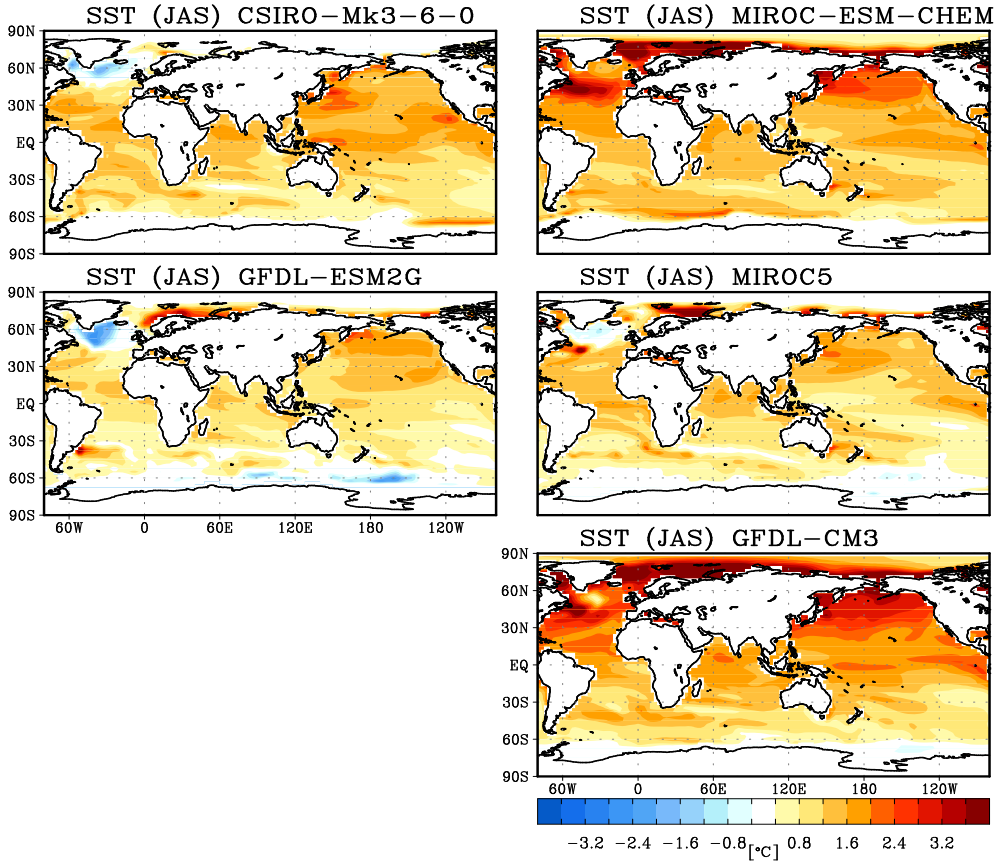

Figure 2.2. SST differences between the 21st century and 20th century for the models producing dry conditions (left panel) and for the models producing wet conditions (right panel) in future Sahel rainfall.

The MIROC models are key to understanding the discrepancy in the future projections because of a strong positive trend of future Sahel rainfall and a strong extratropical SST warming. Thus, the role of NH extratropical SST in predicting future Sahel rainfall is evaluated by reconstructing the simulated rainfall from MIROC-ESM based on different combinations of SST indices. As shown in Figure 1.9, the two commonly-used tropical indices cannot reconstruct the future Sahel rainfall. In contrast, the inclusion of the NH extratropical SST index (0°-360°E, 30°-75°N) in the statistical model reconstructs future Sahel rainfall considerably well, with the strong positive trend similar to the simulated Sahel rainfall (Figure 2.3). Using a single index of NH differential SST warming [(0°-360°E, 30°-75°N) minus (0°-360°E, 20°S-20°N)] in the statistical model also successfully reproduces the strong positive trend (Figure 2.4). Such an improved reproduction of future Sahel rainfall when considering the extratropical SST warming is not found in a similar analysis with a drying model (e.g.

GFDL-ESM2M shown in Figure 2.5, a result that could be expected from the weak future NH extratropical warming simulated by GFDL-ESM2M.

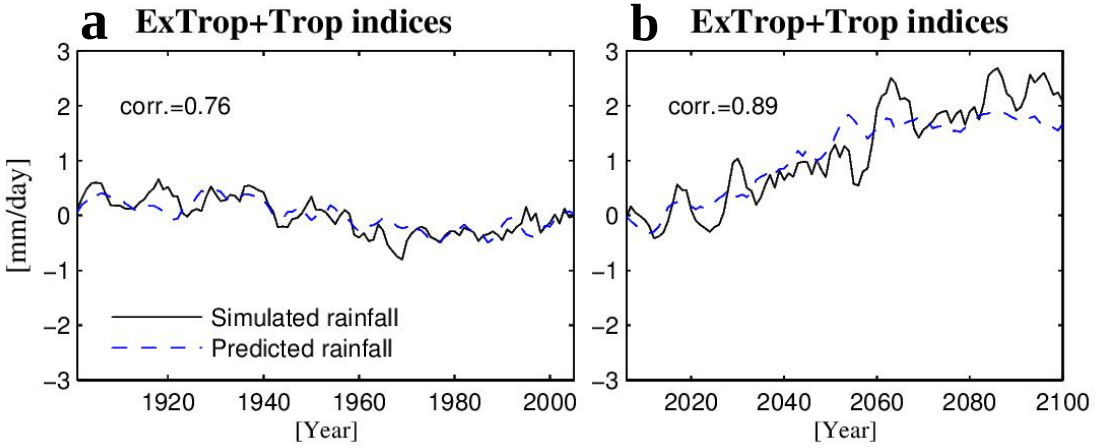

*Figure 2.3. Simulated Sahel rainfalls (black line) from MIROC-ESM and the linearly predicted Sahel rainfall (blue line) based on the three SST indices, two tropical indices (i.e. Atlantic SST gradient and Indo-Pacific SST) and an extratropical SST index, in the (**a**) historical and (**b**) future (RCP4.5) simulations. The coefficients of the multi-linear model are calculated from the historical simulation. All indices are subjected to a five-year running mean.*

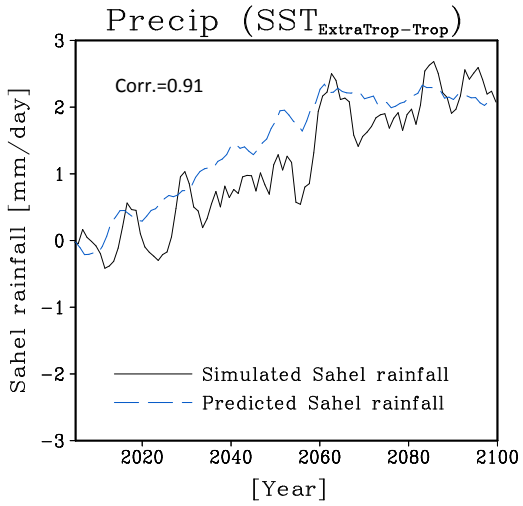

Figure 2.4. Simulated Sahel rainfall (black line) from MIROC-ESM and the linearly predicted Sahel rainfall (blue line) based on a single index defined as the difference between NH extratropical SST and tropical SST [(0°-360°E, 30°-75°N) minus (0°-360°E, 20°S-20°N)].

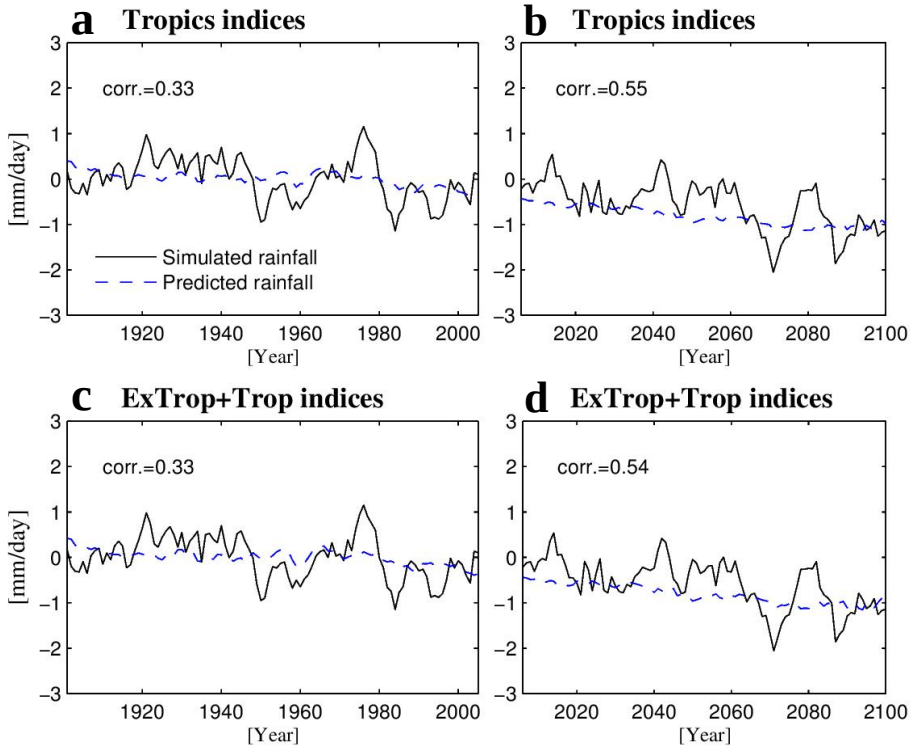

*Figure 2.5. Simulated Sahel rainfalls (black line) from GFDL-ESM2M and the linearly predicted Sahel rainfall (blue line) based on the two tropical SST indices (i.e. Atlantic SST gradient and Indo-Pacific SST) in the (**a**) historical and (**b**) future simulations. **c** and **d** are the same as **a** and **b**, but for using three SST indices including an extratropical SST index to predict Sahel rainfall. All indices are subjected to a five-year running mean.*

Notably, the future development of Sahel rainfall can be reconstructed simply based on 20th century relationships with large-scale SST indices including NH extratropical SST. That is, during the historical period, Sahel rainfall is mainly affected by tropical SSTs because the extratropical SST plays a minor role due to the weak magnitude of its anomalies. However, if the NH extratropical SST warming becomes stronger under a global warming scenario compared to the warming in the tropics, then the future Sahel rainfall changes cannot be explained solely by tropical SST changes. Rather, the extratropical SST should be taken into account.

2.1.3 NH differential warming - future WAM rainfall linkage in CMIP5

The successful reproduction of future rainfall with the inclusion of NH extratropical SST index supports the role of the extratropical warming as a possible origin of the model discrepancy. We further investigate how much the future Sahel rainfall change is related to the NH differential warming across the CMIP5 models. Future changes in Sahel rainfall and those in the NH differential warming are calculated in each CMIP5 model and displayed in a scatter plot (Figure 2.6). Models showing a stronger extratropical warming relative to the tropics tend to project a wetter Sahel. The relationship is quite robust despite other possible factors influencing future Sahel rainfall changes (e.g. local land-surface or land-atmosphere feedbacks, inter-model variations in future tropical SST anomalies, and different model sensitivities to SST forcing). Based on the fitted linear line, the same magnitude of warming over extratropical and tropical oceans leads to drying conditions over the Sahel, which is consistent with a drying Sahel rainfall response to globally uniform warming shown in a previous work (Held et al. 2005).

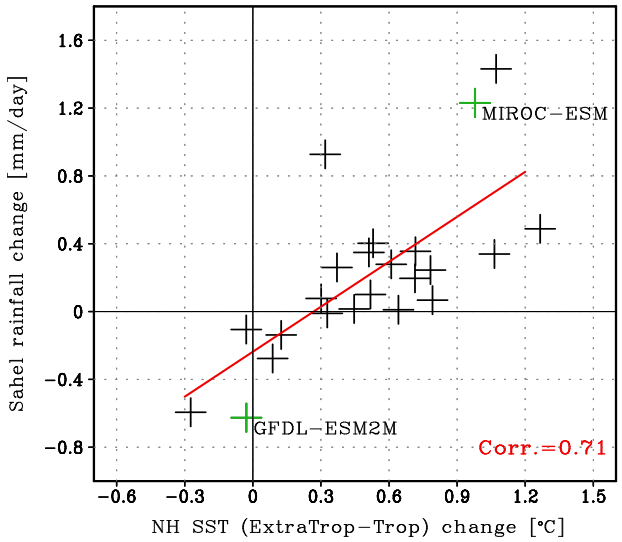

Figure 2.6. Scatter plots of future changes (i.e. mean difference between the twenty-first-century and twentieth-century) in Sahel rainfall versus NH differential warming index across the CMIP5 models: The NH differential warming index is defined by the NH extratropical SST warming relative to tropical warming [(0°-360°E, 30°-75°N) minus (0°-360°E, 20°S-20°N)]. Each mark represents an individual model in CMIP5. The fitted linear-regression lines are shown as red lines.

A similar statistical analysis is conducted with alternative choices of previously known indices, which also include possible extratropical factors associated with Sahel rainfall, such as the global inter-hemispheric SST gradient (Folland et al. 1986) or the SST difference between the subtropical North Atlantic and the global tropical oceans (Giannini et al. 2013). It is found that none of these indices performs comparably well to the NH intra-hemispheric warming index (Figure 2.7a,b). Although the SST index of subtropical North Atlantic minus global tropics shows a comparable correlation with future Sahel rainfall changes, it has some limitations. For example, the relative subtropical index cannot explain the opposite future rainfall anomalies in GFDL-ESM2M and MIROC-ESM, which are key models for diverse future projections. In addition, the subtropical index shows nearly zero rainfall change corresponding to uniform global warming, which is not consistent with previous work showing a drying Sahel in response to globally uniform warming (Held et al. 2005). The regression model with these supplementary indices also shows underperformance in predicting future Sahel rainfall, exhibiting a much weaker positive future rainfall trend than that with our NH differential warming index (cf. Figure 2.4 and Figure 2.7c,d). Taken together, these results highlight the distinct role of NH differential warming for future Sahel rainfall, and the model discrepancy in future Sahel rainfall projections appears to arise from different magnitudes of NH extratropical warming simulated by CMIP5 models.

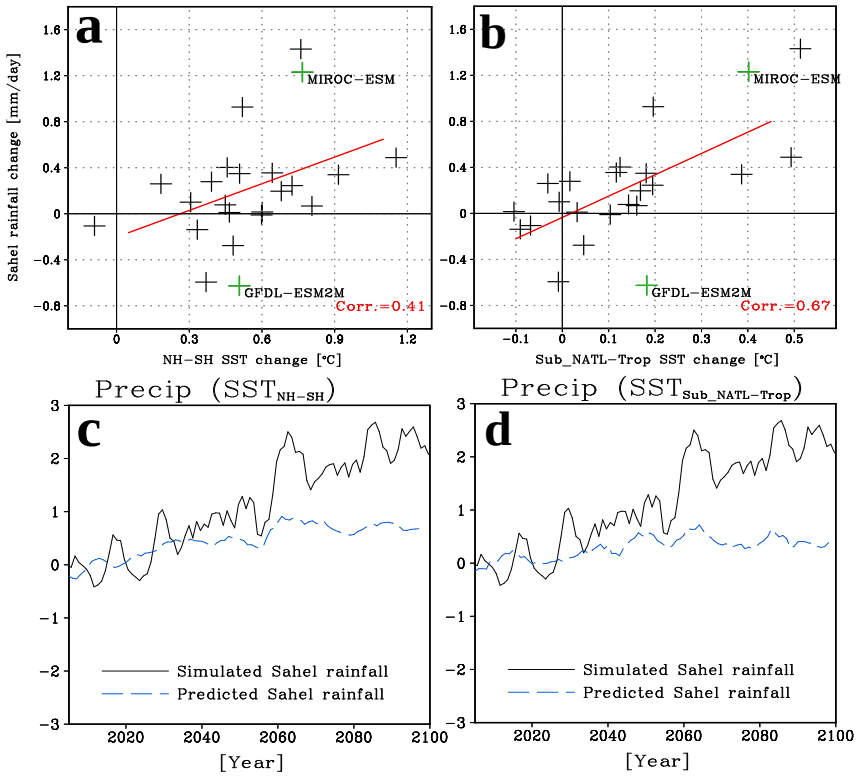

Figure 2.7. ***a-b****, Scatter plots of future changes in Sahel rainfall versus those in two supplementary SST indices across the CMIP5 models: (****a****) global interhemispheric SST gradient [(0°-360°E, 0°-90°N) minus (0°-360°E, 0°-90°S)], and (****b****) difference between subtropical North Atlantic SST and global tropical SST [(75°-15°W, 10°-40°N) minus (0°-360°E, 20°S-20°N)]. Each mark represents an individual model in CMIP5. The fitted linear-regression lines are shown as red lines.* ***c-d****, Simulated Sahel rainfall (black line) from MIROC-ESM and linearly predicted Sahel rainfall (blue line) based on (****c****) the global interhemispheric SST gradient, and (****d****) difference between subtropical North Atlantic SST and global tropical SST.*

2.2 SST sensitivity experiments using ECHAM6

Although the statistical analyses clearly emphasize the role of northern-hemispheric differential heating as a possible source of diverse future projections of Sahel rainfall, we must verify whether the statistical link is physically consistent. Thus, a series of SST-sensitivity experiments with an atmospheric general circulation model (AGCM) has been conducted to yield more robust results and to understand the underlying processes.

2.2.1 Model and experimental design

The ECHAM6 model, developed at the Max Planck Institute for Meteorology, is used for the SST sensitivity experiments. The ECHAM models are known to reproduce the African monsoon reasonably well and have been extensively used for West African Monsoon studies (Bader and Latif 2011; Mohino et al. 2011; Gaetani and Mohino 2013). The model is run at T63 horizontal resolution (1.875° × 1.875°) with 47 vertical levels.

The SST fields prescribed in the model are obtained from two CMIP5 models: GFDL-ESM2M and MIROC-ESM. Note that the corresponding sea ice fields are also used for physical consistency. Each experiment basically consists of a pair of two experiments, named '20C run' and '21C run'. In the 20C run, the model is forced by the monthly climatological mean SSTs over the last thirty years of the 20th century (1970-1999), whereas in the 21C run the model is forced by those over the last thirty years of the 21st century (2070-2099). The precipitation anomalies shown in the present study represent the difference between these two experiments. In the case of isolating the impact of tropical SST, the prescribed SST in the extratropics (poleward of 30°) is fixed to the 20th century SST (as in case in the 20C run), and only the tropical SST (30°S~30°N) from the 21st century is used for the 21C run (and vice versa for the case of extratropical SST). All other boundary conditions (e.g., greenhouse gases and solar radiation) are identical for all integrations. A total of 20 ensemble members with different initial conditions are conducted, and only the JAS mean is shown in this study. A summary of the experimental design is provided in Table 2.1.

Table 2.1. A summary of SST sensitivity experiments. The ECHAM6 model is forced by monthly climatological mean SSTs from MIROC-ESM, and a total of 20 ensemble runs with different initial conditions are carried out. The same experiments are also conducted using GFDL-ESM2M SSTs.

Experiment Name	Prescribed SST (from MIROC-ESM)
MIROC _20C	climatology (1970-1999), global
MIROC_21C	climatology (2070-2099), global

MIROC_21C_tropics	climatology (2070-2999) in tropics (30°S~30°N) + climatology (1970-1999) in extratropics (poleward of 30°N and 30°S)
MIROC_21C_extratropics	climatology (1970-1999) in tropics (30°S~30°N) + climatology (2070-2099) in extratropics (poleward of 30°N and 30°S)

The experiment names used in the main article can be understood as follows.

Exp_MIROC = 'MIROC_21C' – 'MIROC_20C' (Impact of global SST warming)

Exp_MIROC_tropics = 'MIROC_21C_tropics'–'MIROC_20C' (Tropical warming impact)

Exp_MIROC_extratropics = 'MIROC_21C_extratropics'–'MIROC_20C' (Extratropical warming impact)

2.2.2 Performance of ECHAM6 in simulating West African Monsoon

The performance of different versions of ECHAM in reproducing Sahel rainfall has been addressed in several previous studies. For example, ECHAM5 reproduces the observed summer (July-August-September) mean pattern and seasonal cycle of Sahel rainfall reasonably well (Bader and Latif 2011). The historical low-frequency variability of Sahel rainfall can also be accurately reconstructed by prescribing historical SSTs to the model (Mohino et al. 2011). The latest version of ECHAM (ECHAM6), which is used in this study, also shows a good performance in simulating monsoon rainfall (Figure 2.8) and a skilful prediction of Sahel rainfall in the decadal hindcast (Gaetani and Mohino 2013), which will be presented in Figure 4.9. This suggests that ECHAM6 is a reliable tool for a quantitative analysis of the Sahel rainfall.

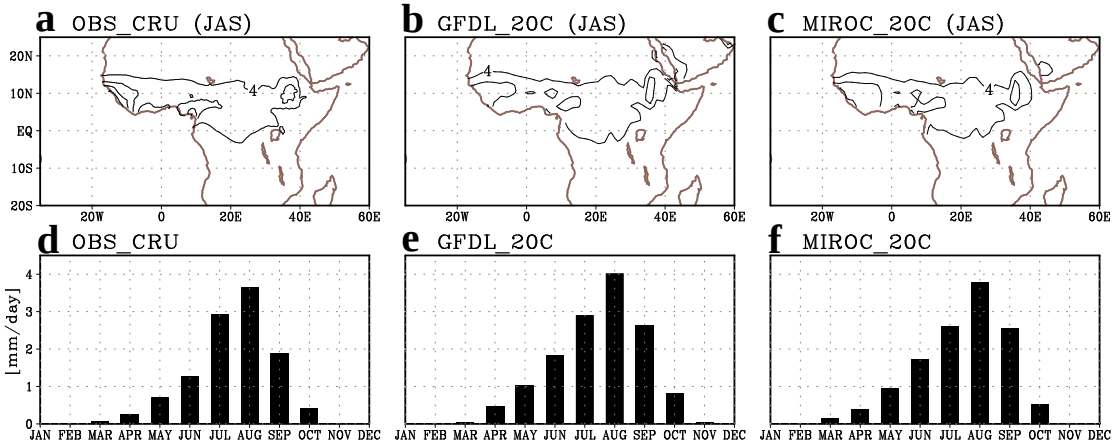

Figure 2.8. ***a-c****, Climatological JAS-mean of Sahel rainfall from (****a****) Climatic Research Unit (CRU) observational data, (****b****) GFDL_20C experiment, and (****c****) MIROC_20C experiment.* ***d-f****, Annual cycle of Sahel rainfall from the same datasets as used in* ***a****-****c****.*

2.2.3 Sahel rainfall responses to future SST warming

The ECHAM6 experiments forced by the global SST warming from GFDL-ESM2M and MIROC-ESM show a significant difference in Sahel rainfall, with a weak Sahel drying in the experiment using GFDL SST and a strong wetting in the MIROC SST case (Figure 2.9a,b). Thus, the AGCM experiment is qualitatively consistent with the drying and wetting Sahel as simulated by GFDL-ESM2M and MIROC-ESM, respectively, in CMIP5. Note that the rainfall responses from our AGCM experiments can be further amplified, if the interactive land and vegetation feedbacks, which are known to increase SST-driven Sahel rainfall changes (Zeng et al. 1999), are included in the experiments. This modelling result highlights the importance of the projected SSTs for the future development of Sahel rainfall and shows that the difference in the projected SSTs can largely explain the divergence of future Sahel rainfall projections. Furthermore, as noted above, the AGCM used for our experiments belongs to one of the CMIP5 models showing neutral conditions for the future Sahel rainfall (Figure 1.8). This condition leads us to hypothesise that different NH future SST anomalies may be a more dominant source of uncertainty in Sahel rainfall projections than different model sensitivities to the same SST forcing, although further experiments performed with a different AGCM are required to test this hypothesis.

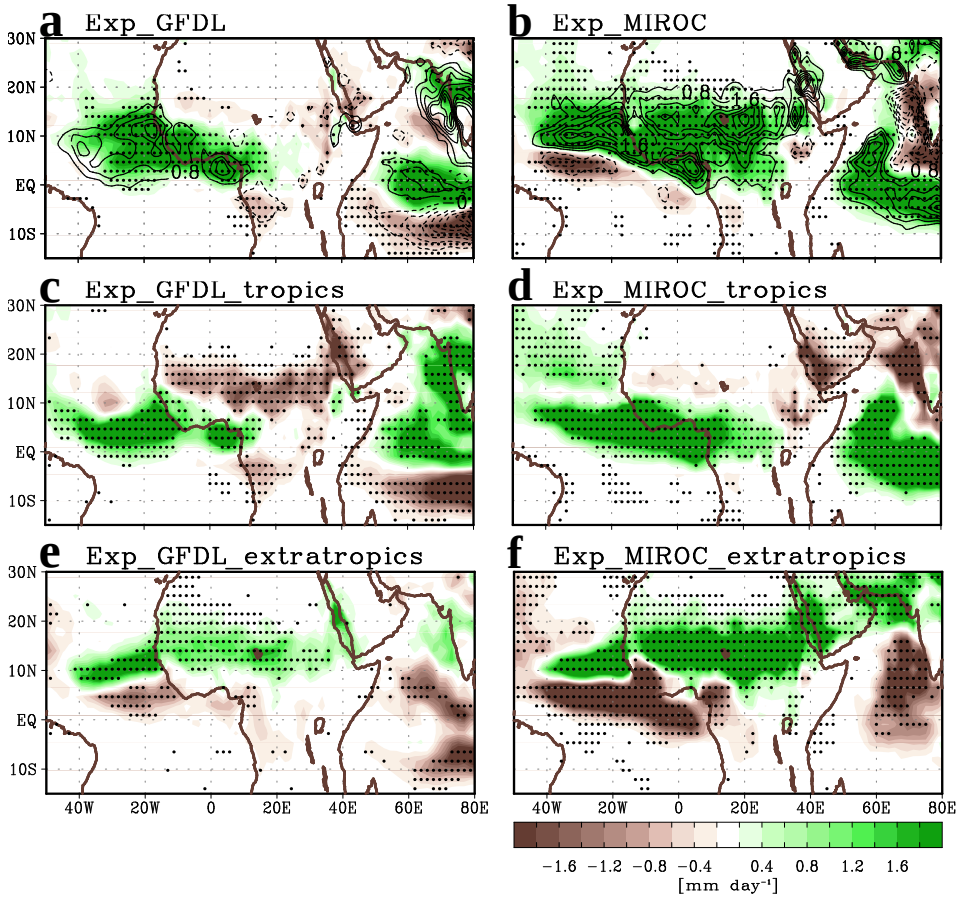

*Figure 2.9. Mean differences in summer (JAS) precipitation between the two experiments: the '21C run' forced by twenty-first century (2070-2099) climatological SST and the '20C run' forced by twentieth century (1970-1999) climatological SST from (**a**) GFDL-ESM2M and (**b**) MIROC-ESM in CMIP5. **c** and **d** are the same as **a** and **b** but for prescribing the twentieth century extratropical SST and the twenty-first century tropical SST for the '21C run'. Similarly, **e** and **f** are precipitation responses when considering the extratropical SST warming only. Contours in **a** and **b** represent the superposition of the precipitation responses from tropical and extratropical SST experiments. The stippled area denotes the 95 % confidence region according to two-tailed t-test.*

Given the successful reproduction of future Sahel rainfall when including future extratropical warming as shown in our previous statistical analysis, the individual impact of extratropical and tropical SST warming on Sahel rainfall needs to be evaluated. To do so, ECHAM6 is forced with the future SST warming restricted to the tropical and extratropical SST parts separately. The interesting finding here is that tropical SST warming induces less precipitation over the Sahel regardless of whether GFDL or MIROC SSTs are used (Figure 2.9c,d). The difference in the magnitude of Sahel drying is presumably due to the varying patterns and magnitudes of tropical

SST anomalies simulated by the two coupled models. For example, the stronger subtropical Atlantic warming in MIROC-ESM than in GFDL-ESM2M may induce less drying over the Sahel by increasing the moisture flux from the Atlantic Ocean. In contrast, both GFDL and MIROC SSTs produce an increase in Sahel rainfall when driven by the extratropical SST warming only (Figure 2.9e-f). In particular, there is a strong wetting over the Sahel when the SSTs from MIROC-ESM are used, which confirms the conclusions of our previous statistical analysis using CMIP5 data. This result suggests that the precipitation decrease in GFDL-ESM2M, which shows less warming in the extratropics, is more affected by tropical warming, whereas the strong precipitation increase in MIROC-ESM is more influenced by strong extratropical warming. In other words, whether a model projects strong wet conditions over the Sahel depends on the dominance of extratropical warming over tropical warming.

Because we argue that the future Sahel rainfall change can be explained by the competition between the two opposing impacts of tropical and extratropical warming, the linearity of the model response is tested. The superposition of two precipitation responses from the tropical and extratropical experiments shows a remarkable similarity to the precipitation response from the global SST warming experiment. This supports the conclusion that the precipitation response to global SST warming in our model experiments can be satisfactorily obtained by the linear combination of precipitation responses to tropical and extratropical SST warming (cf. contours and shadings in Figure 2.9a,b).

The proposed connections linking strong future extratropical warming and Sahel rainfall increase may be relevant to previous findings, particularly focused on the extratropical North Atlantic Ocean. For example, the extratropical North Atlantic cooling associated with Atlantic multi-decadal variability is known to reduce Sahel rainfall by the advection of cold, dry air to North Africa and corresponding changes in sea-level pressure and moist static energy (Liu et al. 2014). The mid-tropospheric Rossby-wave activity originated from the North Atlantic is also a possible atmospheric factor in linking extratropical energy to the African subtropical climate (Barandiaran and Wang 2014). A supplementary AGCM experiment, however, shows that only approximately one-third of the total precipitation increase shown in Figure 2.9f can be

explained by extratropical Atlantic warming alone, indicating that SST warming in other ocean basins, such as the Mediterranean Sea and North Pacific and Arctic Oceans, also contributes substantially to the NH extratropical warming impact on Sahel rainfall.

Our SST-sensitivity experiment does not consider the direct enhanced radiative forcing by CO_2 increase on the continent, and therefore our result might underestimate the impact of CO_2 change on this monsoonal region. In fact, radiative heating by greenhouse gases is generally more prominent over the continent than the nearby oceans during summer due to the smaller heat capacity of the land surface; thus, the West African heat low and corresponding monsoonal flow is intensified, thereby increasing Sahel rainfall (Haarsma et al. 2005; Dong and Sutton 2015). In this regard, it is also informative to examine the direct radiative impact of CO_2 increase (not the impact by changing the SST) on Sahel rainfall. Additional AGCM experiments with increased CO_2 concentration (368 ppm $\rightarrow$ 538 ppm), but prescribed by fixed climatological 20th century SSTs from both GFDL-ESM2M and MIROC-ESM, are conducted to quantify the direct radiative CO_2 impact on Sahel rainfall. The results show that Sahel rainfall is enhanced independently of the GFDL or MIROC SSTs (Figure 2.10), which implies that the direct radiative forcing by CO_2 increase cannot explain the disparate future Sahel rainfall projections. Although the rainfall responses shown here might be slightly overestimated due to the fixed SST boundary condition (i.e., a stronger thermal contrast between ocean and land), the magnitude of the rainfall increase is relatively weak compared to the impact of SST changes, particularly, that of extratropical SST changes (Figure 2.9e,f). Therefore, the direct radiative CO_2 impact cannot be a dominant factor influencing future Sahel rainfall or a source of the model variability in projections of future rainfall.

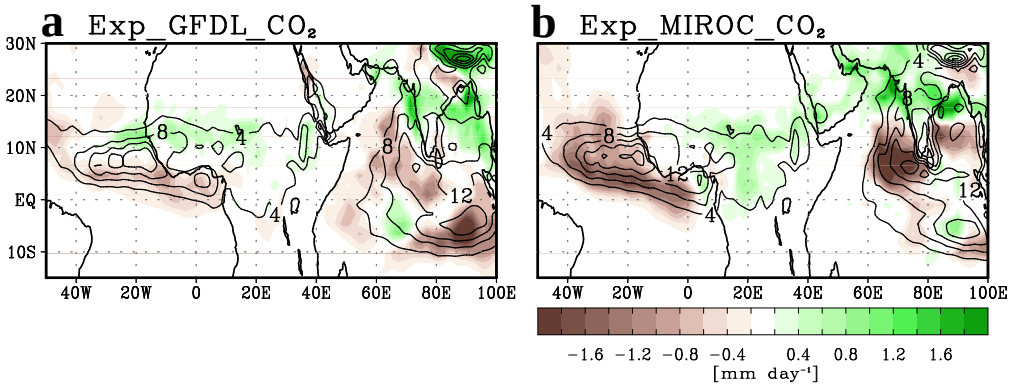

*Figure 2.10. Direct radiative impacts of CO2 increase on Sahel rainfall. Mean differences in JAS-mean precipitation between two experiments prescribing 368 ppm and 538 ppm of CO2 concentration. Both experiments are forced by twentieth century (1970-1999) climatological SST from (**a**) GFDL-ESM2M and (**b**) MIROC-ESM in CMIP5.*

3 Mechanisms of NH differential warming impact on future Sahel rainfall

The previous chapter has shown that the differential warming in the NH is the key to understanding the model discrepancy in future Sahel rainfall. This finding naturally raises a question: **How does the NH differential warming affects future Sahel rainfall?** Given that future Sahel rainfall is explained by the competition between the wetting impact of NH extratropical warming and the drying impact of tropical warming, a mechanistic understanding of future Sahel rainfall change can be obtained by investigating the individual mechanism of tropical and extratropical warming impacts. In this chapter, I pursue that goal by analysing the results from the previous model experiments and performing additional experiments.

3.1 Drying impact of tropical warming

Because of the dominant role of tropical oceans on Sahel rainfall during the historical period (Joly et al. 2007; Biasutti et al. 2008), the mechanisms proposed by previous studies can be applied to explain the relationship between warming tropical oceans and drying Sahel. Such mechanisms include the reduced ascent at certain convective margins due to the higher moisture requirement for convective instability,

so-called “upped-ante mechanism” (Neelin et al. 2003; Chou and Neelin 2004), and the anomalous subsidence over the Sahel caused by tropical ocean warming (Sobel et al. 2002; Bader and Latif 2003; Herceg et al. 2007). By analysing the tropical warming experiment, ‘Exp_GFDL_Tropics’, which has shown a significant drying over the Sahel (Figure 3.1), we check how these mechanisms explain the Sahel drying under tropical warming.

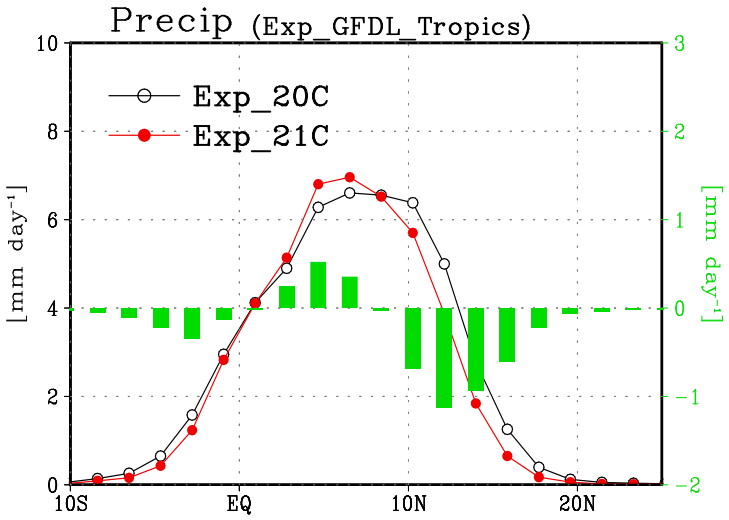

Figure 3.1. Zonally-averaged (10W°-30°E) precipitation from the experiment ‘GFDL_20C’ (black line) and ‘GFDL_21C_tropics’ (red line). Bar graph represents the difference between the two experiments (GFDL_21C_tropics minus GFDL_20C).

3.1.1 Insufficient increase in moist static energy

The Sahel region is located at the northern edge of tropical rain belt over the Africa. When the tropical troposphere becomes warmer in a warming climate, the atmospheric boundary layer must have a sufficient increase in moist static energy[2] to meet the requirement for a continuous convection in this region. This extra moist static energy mostly comes from additional moisture, but it is not easy to meet the convection requirement over the Sahel region where the prevailing north-easterly 'Harmattan' winds blow from the arid northern region, Sahara. On the other hand, the moisture supply at the center of convective region is relatively sufficient due to its

[2] Moist static energy is defined as $C_p \cdot T + g \cdot z + L_v \cdot q$, where C_p is specific heat capacity, T is absolute temperature of air, g is the gravitational constant, z is geopotential height, Lv is the latent heat of vaporization, and q is specific humidity

location near to the ocean, thus the high humidity can lead to increased convection. In fact, the increase in moist static energy by tropical warming is not high over the Sahel region (10°-20°N) compared to the tropical rain band over the Africa (Figure 3.2). Eventually, the rainfall increases near the center of convective regions but decreases at the marginal region. This 'wet-get-wetter and dry-get-drier' relationship is well represented in the rainfall response to tropical warming as shown in Figure 3.1.

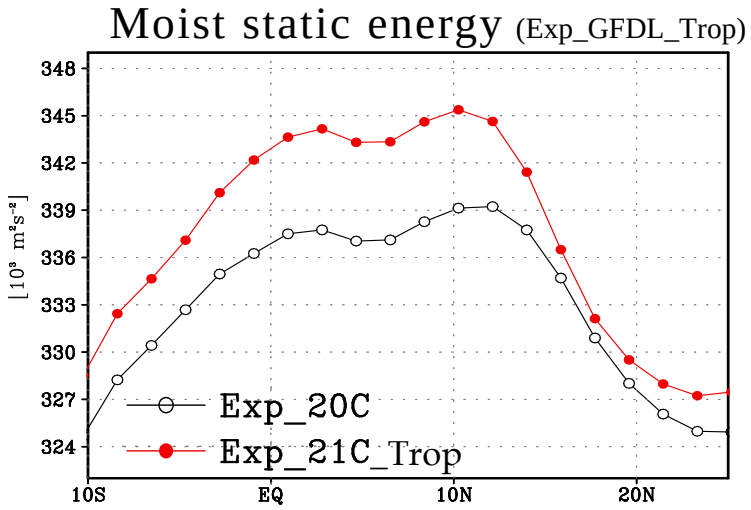

Figure 3.2. Zonally-averaged (10W°-30°E) moist static energy at 1000hPa simulated from the experiment 'GFDL_20C' (black line) and 'GFDL_21C_tropics' (red line).

3.1.2 Stabilized tropical troposphere

Tropical warming generally leads to a strong temperature increase in the upper troposphere. Fast equatorial waves conveys the warming to the whole upper troposphere in the tropics and flattens horizontal temperature gradient. This causes the decrease in convective instability in the tropical troposphere, which is similar to an El Nino response. The tropical warming experiment performed in the previous chapter also shows the warmer temperature anomalies in the upper level, indicating the stabilized atmosphere (Figure 3.3). Together with the insufficient moist static energy increase over the Sahel, this stabilized atmosphere provides an unfavourable condition for the Sahel rainfall increase. Overall results show that the drying Sahel by tropical warming is well explained by the previously-known mechanisms on how tropical warming changes the pattern of tropical rainfall.

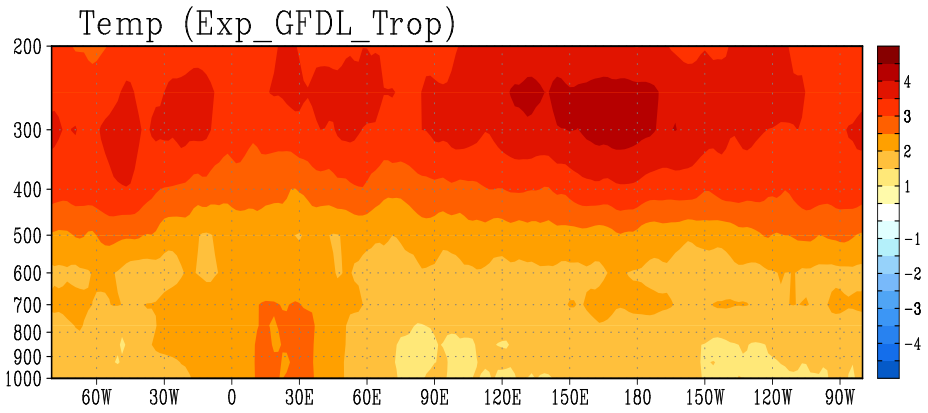

Figure 3.3. Stabilized tropical atmosphere caused by tropical SST anomalies. The JAS mean tropical (20°S-20°N) air temperature anomalies (unit: °C) in response to tropical SST warming.

3.2 Wetting impact of NH extratropical warming

In contrast to the impact of tropical warming, the role of extratropical SST warming on the Sahel rainfall has been relatively less studied. One might argue that the global interhemispheric thermal gradient generated by the strong NH extratropical warming is an extratropical factor inducing the Sahel rainfall increase by shifting the tropical rainbelt to the north (Broccoli et al. 2006; Kang et al. 2008). However, the zonal mean precipitation change in the extratropical warming experiment clearly indicates that the Sahel rainfall increase is only partially explained by a northward rainbelt shift, and more important factors associated with the Sahel rainfall intensity change are involved given the meridionally asymmetric rainfall anomalies (Figure 3.4). Thus, we suggest potential mechanisms for how the NH differential warming is linked to the increase in Sahel rainfall by further analysing the strong extratropical warming experiment (Exp_MIROC_extratropics).

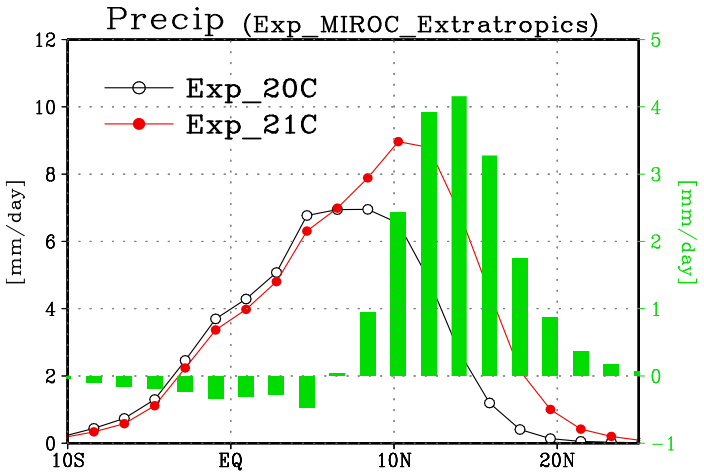

Figure 3.4. Zonally-averaged (10W°-30°E) precipitation from the experiment 'MIROC_20C' (black line) and 'MIROC_21C_extratropics' (red line). Bar graph represents the difference between the two experiments (MIROC_21C_extratropics minus MIROC_20C).

3.2.1 Increased moisture inflow

One factor is the increased moisture flux from adjacent oceans, such as tropical Atlantic and Mediterranean Sea (Figure 3.5). Given the climatological mean state exhibiting south-westerly and north-easterly moisture fluxes that lead to the convergence over the Sahel, the moisture flux anomalies in Figure 3.5 indicate the strengthening of monsoonal flow. In particular, the large-scale low pressure anomaly can deepen the Sahara Low, known as a main driver of the West Africa monsoonal wind, and thus intensify the westerly flow over the tropical Atlantic Ocean and West Africa. Consequently, the anomalous westerly moisture flux enhances moisture convergence over the Sahel, and in turn increases the rainfall. Given this connection between the NH extratropical warming and Sahel rainfall increase, our results are consistent with previous works. For example, one study showed that the increased temperature and atmospheric humidity advected from the extratropics can induce a positive long-wave radiation moisture feedback and either maintain or further amplify the surface warming over North Africa (Liu et al. 2014). This finding provides a favourable condition for the Sahel rainfall increase due to the strengthening of the land-sea thermal contrast (associated with a strong monsoon flow) and the increased moist static energy (associated with a northward shift of the climatological rainbelt) (Chou et al. 2001; Liu et al. 2014). Another study suggested the role of the Sahara Low

as a possible source of the variation in future Sahel rainfall projections (Biasutti et al. 2009). The disparate magnitudes of NH differential warming emphasised in the present study may be an underlying cause of the different Sahara Low intensities projected by climate models, leading to the diverse projections of Sahel rainfall.

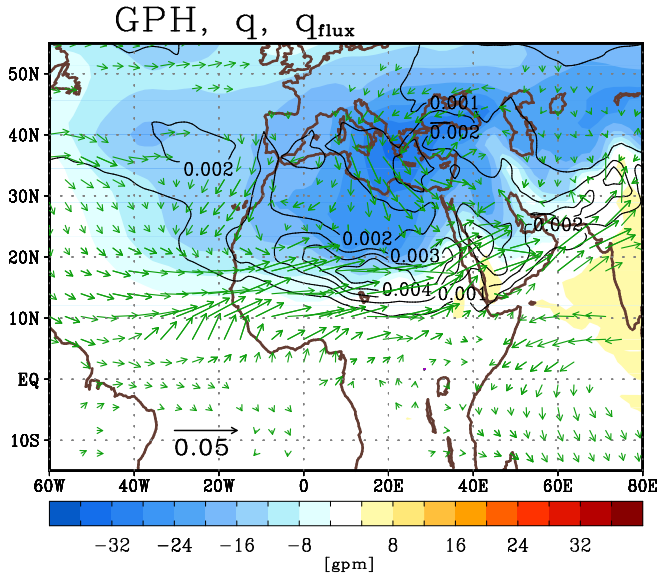

Figure 3.5. The JAS-mean difference in 925-hPa geopotential height (shadings), moisture (contours), and moisture flux (arrows) between the two experiments, MIROC_21C_extratropics and MIROC_20C. The difference in moisture flux (kg_{H2O} kg_{air}^{-1}·m s^{-1}) is only plotted where the mean difference is statistically significant, exceeding the 95% confidence level according to a two-tailed t-test.

Similar to the circulation change over North Africa caused by the NH extratropical warming, tropical Atlantic SST warming can also result in an increase in Sahel rainfall with the intensification of the Sahara heat low and the increased low-level moisture flux (Sutton and Hodson 2007; Martin et al. 2014). However, the wetting impact of the specific warming pattern in the tropics is relatively weak in a warming climate, thus the drying impact by the warming of the Indian and Pacific oceans dominates the Sahel rainfall response as shown in our tropical SST experiments (e.g. Figure 2.9c,d). Specifically, if the future extratropical warming is stronger than the tropical warming, the extratropical impact on the Sahara Low or Sahel rainfall is expected to dominate subtropical/tropical impacts. A previous modelling work based on the historical period also supports this relation, showing that tropical part of NH Atlantic warming

cannot give a dominant contribution to the Sahel rainfall increase responding to the whole NH Atlantic warming (Sutton and Hodson, 2007).

3.2.2 Upper-level circulation changes

Another possible link between the NH differential warming and the increase in Sahel rainfall can be found in upper-level jets over Africa. Two tropical jets, the Tropical Easterly Jet (TEJ) and the African Easterly Jet (AEJ), are upper-level circulation factors known to influence Sahel rainfall (Nicholson 2009b). The intensity of the TEJ, which modulates the divergence and uplift in the upper troposphere, is associated with rainfall anomalies over much of western Africa (Pattanaik and Satyan 2000; Grist and Nicholson 2001; Nicholson 2008), and the location of the AEJ is linked to the latitudinal extent of the atmospheric ascent and the tropical rainbelt over West Africa (Grist and Nicholson 2001; Nicholson 2009b). It is found that the responses of these two jets in our extratropical warming experiment are in agreement with the observed relationship between the jets and Sahel rainfall. The TEJ is significantly intensified in the presence of extratropical warming, whereas the AEJ shifts northward by approximately 4° over the Sahel region with relatively little change in its magnitude (Figure 3.6). Such circulation features are consistent with the anomalous ascending motion over the Sahel and the corresponding rainfall increase (Figure 3.6 and Figure 3.7a).

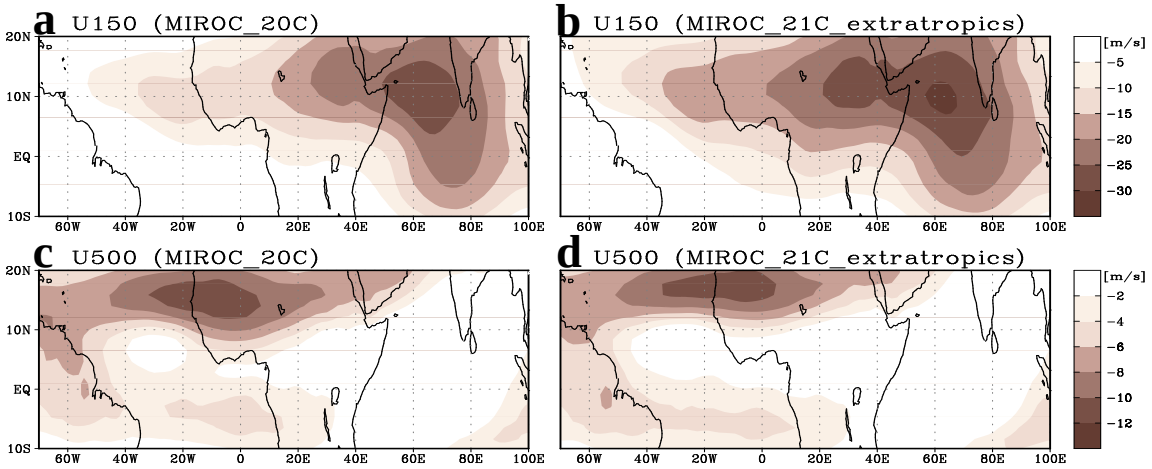

*Figure 3.6. The JAS-mean zonal wind at 150hPa from the experiment 'MIROC_20C' (**a**) and 'MIROC_21C_extratropics' (**b**). **c** and **d** are the same as **a** and **b** but for 500hPa zonal wind.*

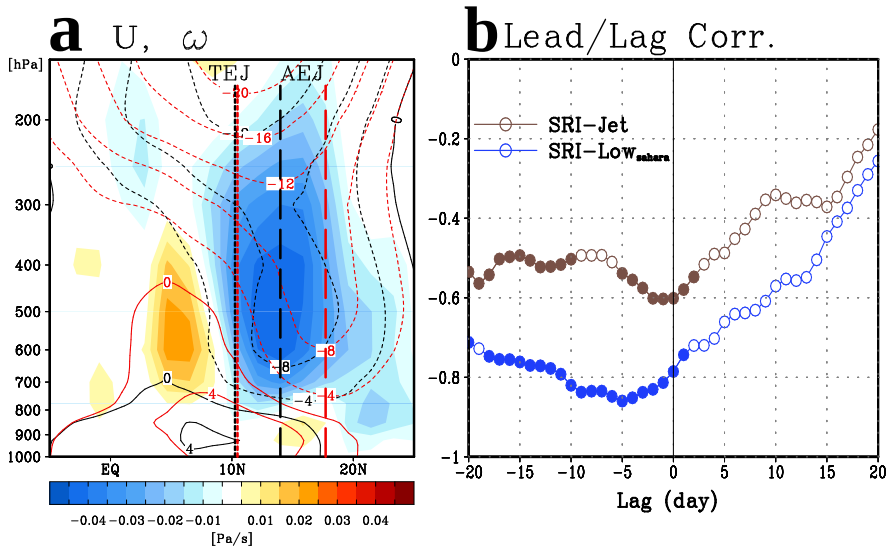

Figure 3.7. ***a****, Zonally-averaged (10°W-30°E) zonal wind from MIROC_20C (black contours) and MIROC_21C_extratropics (red contours). Vertical lines represent axes of tropical easterly jet (dotted lines) and African easterly jet (dashed lines) for MIROC_20C (black) and for MIROC_21C_extratropics (red). Shading represents the JAS mean difference between MIROC_21C_extratropics and MIROC_20C.* ***b****, Lead/Lag correlations between Sahel rainfall (10°W-30°E; 10°-20°N) and Sahara Low (10°W-30°E; 20°-30°N) and between Sahel rainfall and upper level tropical easterly jet (10°W-30°E; 5°-15°N). The ensemble-mean daily data is used for this analysis. Negative lag indicates that Sahara Low and jets lead the Sahel rainfall. Filled circles represent correlations exceeding 90% confidence level.*

The aforementioned mechanism of the NH extratropical warming impact is physically plausible and is consistent with previous observational results. However, it does not provide clear evidence of causal relationships. For example, changes in the Sahara Low or the upper-level jet might be caused by the increased precipitation. To clarify this uncertainty, both the lead-lag relationships between Sahel rainfall and the strength of Sahara Low, and between Sahel rainfall and the intensity of TEJ were analysed by using daily model outputs (Figure 3.7b). It is found that the changes both in the Sahara Low and jet strength generally precede Sahel rainfall change. Therefore, the change in atmospheric dynamics is likely to be a cause, rather than a consequence, of the substantial increase in Sahel rainfall.

3.2.3 Contribution of different NH extratropical ocean basins

Although the large-scale moisture and circulation changes associated with the NH extratropical warming are physically consistent with the Sahel rainfall increase, a detailed mechanism still needs to be elucidated. One way to do that is to find a key SST area in the relationship between the NH extratropical warming and Sahel rainfall increase. Similar to the SST sensitivity experiments shown in the previous chapter, the SST forcing is further restricted to different ocean basins and quantify the relative importance of different ocean basins.

The AGCM experiment forced by the projected future SST warming from MIROC-ESM shows that the future Sahel rainfall increase mostly results from the NH extratropical SST warming as expected from Figure 2.9f (Figure 3.8). To understand the detailed extratropical SST-Sahel rainfall relationship, which is the key for the future Sahel rainfall increase, the NH extratropical forcing used in the AGCM experiment is further separated into four different ocean basins, Arctic, North Atlantic, North Pacific, and Mediterranean Sea. This separation of SST forcing is based on previous studies that show a clear linkage of Sahel rainfall changes to North Atlantic SST and Mediterranean (Rowell 2003; 2013; Liu et al. 2014). The rainfall responses show that the Mediterranean warming is the most dominant contributor to the future Sahel wetting. The wetting impact of North Atlantic warming contributes the second most despite its stronger warming than the Mediterranean warming. Warming in the Arctic and North Pacific oceans contributes only a minor impact to the future Sahel wetting.

The relatively minor impacts of warming in other NH extratropical oceans may be contradicting to a common belief that the global-scale ITCZ shift is the key mechanism in the linkage between an interhemispheric thermal gradient and Sahel rainfall changes. That is, previous studies often relate the interhemispheric asymmetry of global SST anomaly to Sahel rainfall changes due to the characteristics of ITCZ location shifting towards a warmer hemisphere (Chiang and Friedman 2012). As shown here, however, although there is a strong warming in the Northern Hemisphere, its impact is not dominant compared to the wetting impact of the Mediterranean Sea warming.

This implies that the previously-known ITCZ shift mechanism may not be the main cause of the increased future Sahel rainfall, but rather the Mediterranean impact mostly contributes to the link between the future interhemispheric differential warming and Sahel rainfall. This will be further examined in Chapter 5.

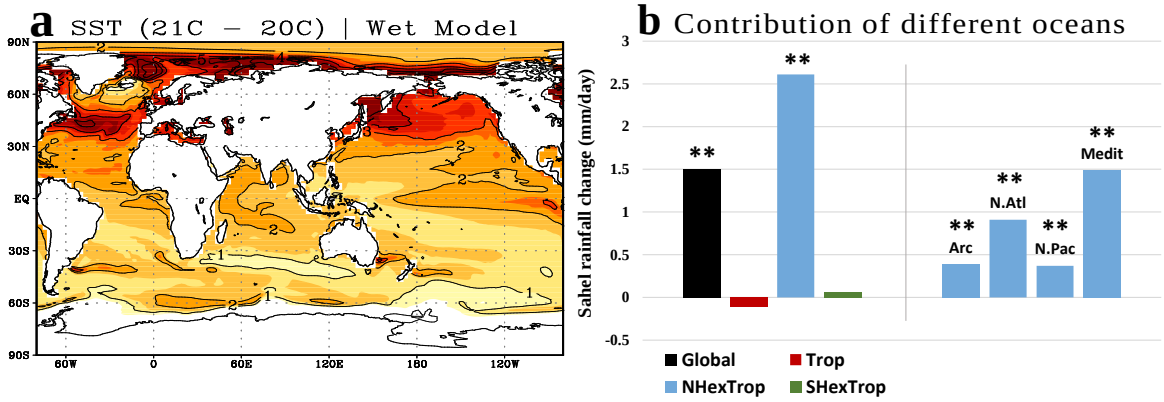

Figure 3.8. ***a****, Summer mean SST difference between the twenty-first and twentieth century simulated by MIROC-ESM that projects a strong future Sahel wetting.* ***b****, Simulated summer Sahel rainfall responses forced by global (black), tropical (red, 30°S -30°N), NH extratropical (blue, 30°-75°N), and SH extratropical (green, 30°-75°S) SST anomalies in* ***a****. The NH extratropical impact is subdivided into four different NH extratropical ocean basins, Arctic (0°-360°E, 65°-90°N), North Atlantic (100°W-0°, 30°-65°N), North Pacific (60° E-100°W, 30°-65°N), and Mediterranean Sea (0°-50°E, 30°-50°N). The significant rainfall responses are marked by single asterisk (*) indicating P < 0.10 and by double asterisks (**) indicating P < 0.05.*

4 Emerging impact of Mediterranean Sea in a warming climate

The dominant impact of Mediterranean warming found in our previous extratropical warming experiments may provide an important clue about how Sahel rainfall will change under greenhouse warming. This is particularly important if the warming in the extratropics continues as projected by most climate models. In this chapter, **we will examine in more detail about how the Mediterranean Sea impact is changing as its warming increases** and **how much the future Mediterranean warming can explain the different future Sahel rainfall projections**. It is also examined whether the dominant role of future Mediterranean warming is also found in the recent observed period. [3]

4.1 Increasing role of Mediterranean Sea in the future

To understand the first-order response of Sahel rainfall to future extratropical warming, additional SST sensitivity experiments are performed by applying various magnitudes of uniform warming in different extratropical ocean basins. The model response shows that the Mediterranean impact on Sahel rainfall turns out to be the

3 This chapter is based on the following paper: Park, J.-Y., J. Bader, and D. Matei, 2015: Anthropogenic Mediterranean warming essential driver for present and future Sahel rainfall. *Nature Climate Change, under review*.

dominant factor, with a strong Sahel rainfall response proportionally increased with the magnitude of SST warming (Figure 4.1). The North Atlantic warming generally shows a weaker impact on Sahel rainfall compared to the Mediterranean warming, with a linearly increasing rainfall response to weak SST warming but a somewhat steady response to strong SST warming. The saturation of the North Atlantic impact may be due to its indirect influence on Sahel rainfall by the advection of moisture and temperature towards the Northern Africa (Liu et al. 2014) and/or by the northward shift of ITCZ due to the homogenized temperature response in the NH extratropics (Kang et al. 2014).

The other ocean basins, Arctic and North Pacific, however, do not exhibit such a distinct Sahel rainfall response to different magnitudes of SST warming. This result again supports that the ITCZ shift effect may not play a dominant role in increasing Sahel rainfall increase under the NH extratropical warming. Overall results here suggest that the wetting impact of Mediterranean warming may become more important as global warming progresses, particularly when future extratropical warming is greater than tropical warming. Therefore, the future Sahel rainfall can be substantially modified by different magnitudes of future Mediterranean warming.

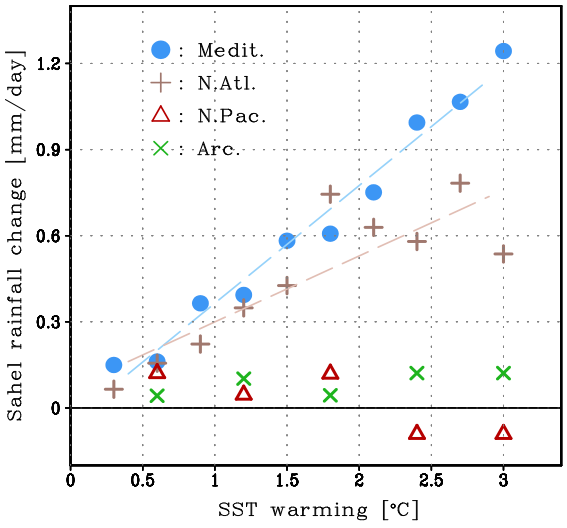

Figure 4.1. Sahel rainfall responses to different magnitudes of uniform warming in the individual NH extratropical ocean basin, Mediterranean, North Atlantic, North Pacific, and Arctic oceans.

A key issue in West African Monsoon research is a large uncertainty in future Sahel rainfall projections (Cook and Vizy 2006; Biasutti et al. 2008). As shown in Chapter 1, different climate models disagree even on the sign of the future Sahel rainfall trend. Given the potentially dominant effect of the Mediterranean Sea in a warming climate, it is worth to examine whether different future Mediterranean warming can explain the future Sahel rainfall uncertainty. A multi-model analysis reveals that different magnitudes of future Mediterranean warming is closely correlated with diverse future Sahel rainfall projections across the climate models (Figure 4.2). In particular, the relationship becomes more obvious when considering the relative Mediterranean warming compared to tropical SST warming in that the wetting impact by Mediterranean warming potentially competes with the drying impact by overall tropical warming in the future (Figure 4.3). Such a successful explanation of the future Sahel rainfall uncertainty implies that the disparate Mediterranean warming simulated by current climate models is a crucial source of the future uncertainty despite other possible factors influencing future Sahel rainfall (e.g. intermodal variations in land surface process, detailed pattern of future SST anomalies, and model sensitivity to SST forcing). This result is consistent with the finding in Chapter 2 that suggests future NH differential warming as a key to understanding the discrepancy in future Sahel rainfall projections (Park et al. 2014), but further elucidating a key SST area in the pathway of the NH differential warming impact on future Sahel rainfall

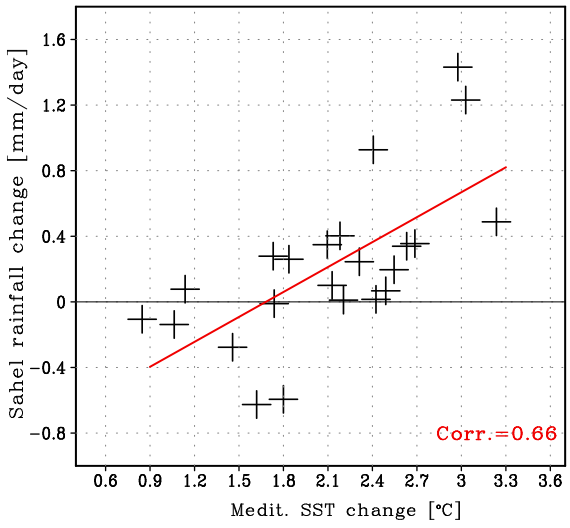

Figure 4.2. Scatter plots of future changes (i.e. mean difference between the twenty-first-century and twentieth-century) in Sahel rainfall versus Mediterranean SST across the CMIP5

models. Each mark represents an individual model in CMIP5. The fitted linear-regression line is shown as red line and the correlation coefficient is significant at P < 0.01.

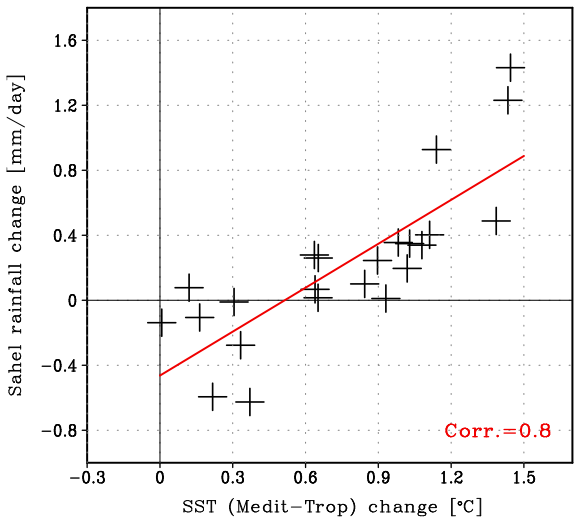

Figure 4.3. Same as Figure 4.2 but against future Mediterranean SST change relative to tropical SST change.

4.2 Evidences in the observed period.

Considering the recent warming signals in global oceans and the recent increasing trend of Sahel rainfall, the emerging impact of the Mediterranean Sea may also leave a footprint on the recent observational record. In fact, the extensive research has shown that the severe Sahel drying trend during 1950-1990 is dominated by tropical SST changes, whereas the cause of the recent wetting trend since the 1990s has not been elucidated. Rather, the same mechanism causing the past Sahel drought is often assumed to hold for the recent wetting trend. Given the worldwide climate shifts frequently reported in recent decades (Hakkinen and Rhines 2004; Kwon et al. 2007; Park et al. 2012) and the time-varying SST-Sahel relationship depending on the global mean climate (Biasutti et al. 2008), however, the previously-known pathway of SST impact on Sahel rainfall would have been changed in the recent warming period. Therefore, in this section, we will investigate whether the dominant role of the Mediterranean Sea in controlling Sahel rainfall can be found in the recent period.

4.2.1 Sahel rainfall increase and associated SST anomalies

Since the 1970s, summer Sahel rainfall shows a marked contrast with a drying condition until the mid-1980s and a wet condition (or a recovery) afterward (Figure 4.4a). The composite difference of SST between wet and dry years exhibits an interhemispheric contrast of SST anomalies, including positive north-south SST gradient across the tropical Atlantic and cooling in the Indian Ocean and eastern Pacific (Figure 4.4b). This SST pattern is robust even when using the precipitation and SST data from different observational products and generally consistent with the SST difference between wet years in the 1950/60s and dry years in the 1970/80s (Folland et al. 1986). For example, the global SST pattern associated with the past wet conditions over the Sahel, such as a "warm Northern Hemisphere (NH) and cold Southern Hemisphere (SH)" pattern and a cooling over the Indian Ocean and eastern Pacific, seems to be able to explain the recent wet conditions (Figure 4.5b). Thus, it might be tempting to conclude that the same mechanism governing the past Sahel rainfall change holds for the recent period of Sahel wetting. However, the magnitudes of SST anomalies in the tropics, a key area for understanding Sahel rainfall variations until mid-1980s, are still quite different in the past and recent periods. Moreover, even the same magnitude of SST anomalies may trigger different atmospheric teleconnections of SST impact due to the recent tropical warming trend, suggesting the necessity of careful examination of the recent SST-Sahel relationship.

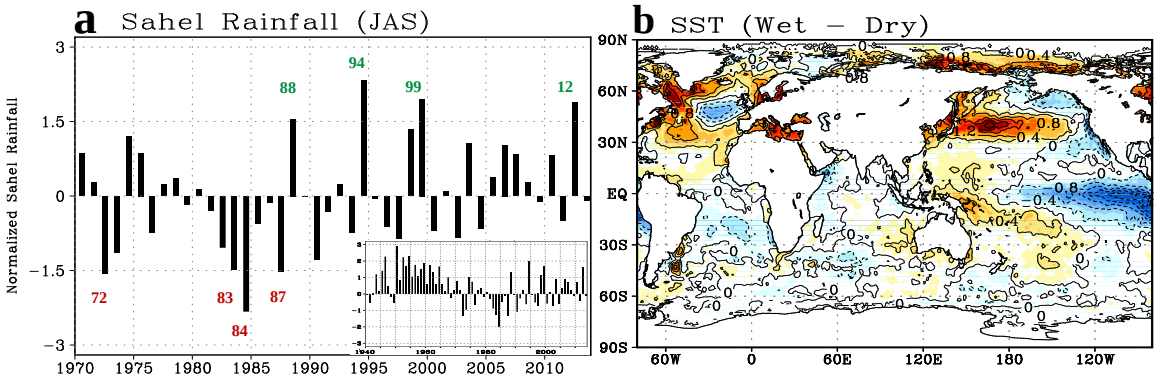

*Figure 4.4. **a**, Time series of observed JAS-mean rainfall anomalies over the Sahel (10°W-30°E; 10°-20°N) during the period 1970-2013. The wet and dry years are identified by rainfall anomalies exceeding ±1.5 standard deviation. The bottom right plot represents the historical*

*Sahel rainfall anomalies during 1940-2013. **b**, Composite mean difference of summer SSTs between the wet and dry years in the Sahel region.*

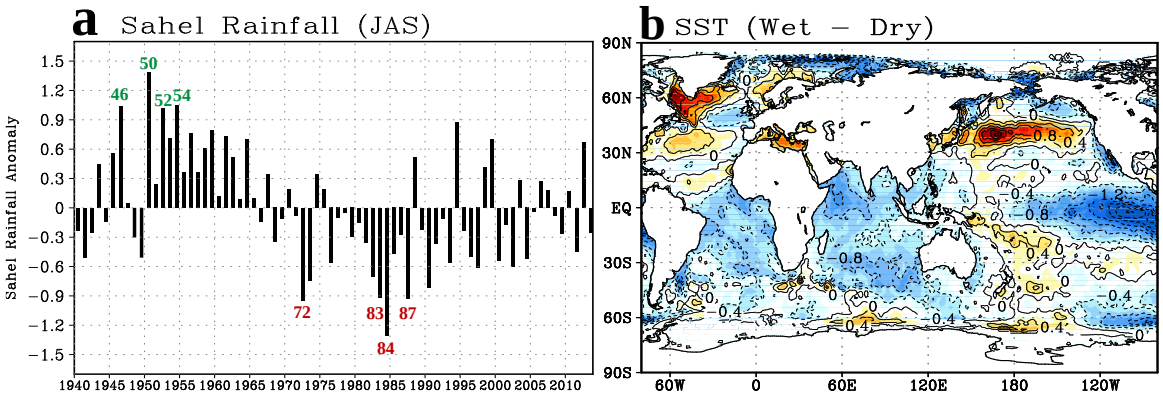

Figure 4.5. Same as Figure 4.4 but during the period 1940-2013. The wet and dry years are identified by rainfall anomalies exceeding ±0.9 mm day^{-1}.

4.2.2 Dominant Mediterranean Sea impact on observed Sahel wetting

The role of the recent SST changes in forcing the Sahel wetting is investigated by performing a series of SST-sensitivity experiments with the ECHAM6. Similar to the experiments shown in Figure 3.8, the atmospheric response to the composite SST anomalies associated with the recent Sahel wetting is defined as the difference between ensemble mean of two experiments, the SST perturbed run and the control run. The 1979-2008 climatological SSTs used in the Atmospheric Model Intercomparison Project (AMIP2) are prescribed in the control run, while the composite SST anomalies overlaid with the AMIP2 SST are prescribed in the perturbed run.

The modelled rainfall response to the global SST anomalies in Figure 4.4b shows a significant increase in Sahel rainfall (Figure 4.6). This indicates that the recent Sahel wetting is largely driven by SST changes, which may support the previously-known wetting effect of the positive north-south tropical Atlantic gradient and Indo-Pacific cooling. However, further experiments forced by the composite SST anomalies restricted to the tropics and extratropics suggests that the recent Sahel rainfall increase mostly results from the extratropical SST anomalies, not from the tropical SST patterns.

In fact, the tropical SST anomalies turn out to have a significant drying impact on the Sahel. This result differs from earlier studies in that forcing from the tropical oceans, such as tropical Atlantic, Indian and Pacific oceans, may not always be dominant in driving historical Sahel rainfall variations (Lu and Delworth 2005).

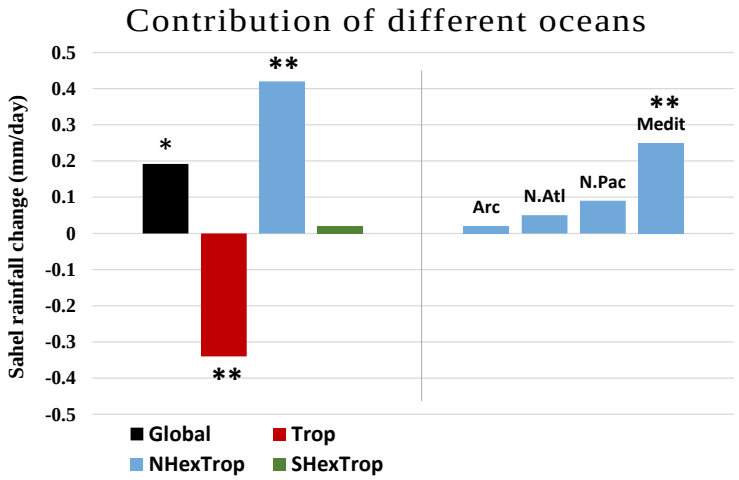

Figure 4.6. Simulated JAS-mean Sahel rainfall responses forced by global (black), tropical (red, 30°S -30°N), NH extratropical (blue, 30°-75°N), and SH extratropical (green, 30°-75°S) SST anomalies related to the recent Sahel rainfall increase. The NH extratropical impact is subdivided into four different NH extratropical ocean basins, Arctic (0°-360°E, 65°-90°N), North Atlantic (100°W-0°, 30°-65°N), North Pacific (60° E-100°W, 30°-65°N), and Mediterranean Sea (0°-50°E, 30°-50°N). The significant rainfall responses are marked by single asterisk (*) indicating P < 0.10 and by double asterisks (**) indicating P < 0.05.

Such inconsistency in the past and recent relationships between tropical SST and Sahel rainfall is caused by a different atmospheric teleconnection under a warming tropical climate. In the past Sahel wet period, anomalous cooling in the Indian Ocean and eastern Pacific reduces vertical stability of tropical atmosphere by decreasing moist static energy at upper levels, provides a favorable condition for large-scale convection over tropical continents, and consequently leads to an increase in Sahel rainfall (Janicot et al. 1996; Bader and Latif 2011). However, in the recent Sahel wet period, the center of convective region that controls tropical atmospheric stability is shifted to the western Pacific Warm Pool region. That is, the tropical atmospheric response to the grand La-Nina-like pattern change (warming in the western Pacific and cooling in the eastern Pacific) shows that the stabilizing impact, or equivalently drying impact, of western Pacific warming dominates the wetting impact of SST

changes in other tropical ocean basins (Figure 4.7). This modified tropical SST-Sahel teleconnection is quite similar to the feature shown in Figure 3.3 and presumably due to different sensitivity of tropical convection caused by a marked Warm Pool warming in recent decades (Park et al. 2012).

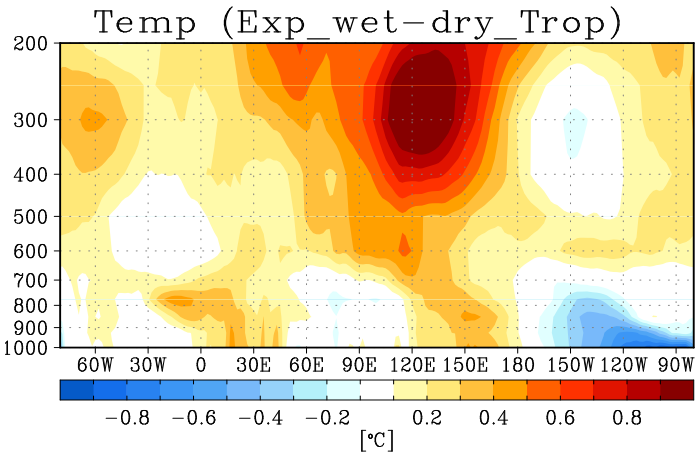

Figure 4.7. The JAS-mean tropical air temperature anomalies (longitudinally averaged between 20°S and 20°N) in response to tropical SST changes shown in Figure 4.4b.

The wetting impact of the NH extratropical SST changes, the key for the recent Sahel rainfall increase, is further analysed. Similar to the further separation of SST forcing as shown in the previous chapter, the NH extratropical forcing used in the AGCM experiment is restricted to four different ocean basins, Arctic, North Atlantic, North Pacific, and Mediterranean Sea. The model responses show that the Mediterranean warming is the most dominant contributor to the recent Sahel wetting (Figure 4.6). Forcing from other ocean basins, however, contributes only a minor portion of the Sahel wetting despite their large portion of NH extratropical ocean areas. The model responses found here are still consistent even when using the boundary SST forcing defined by the mean difference between earlier dry period (1970-1985) and later wet period (1994-2013) instead of the composite SST in Figure 4.4b (Figure 4.8). Overall outputs from the AGCM experiments forced by recent SST changes are consistent with our previous results and further support the emerging role of the Mediterranean Sea in a warming climate.

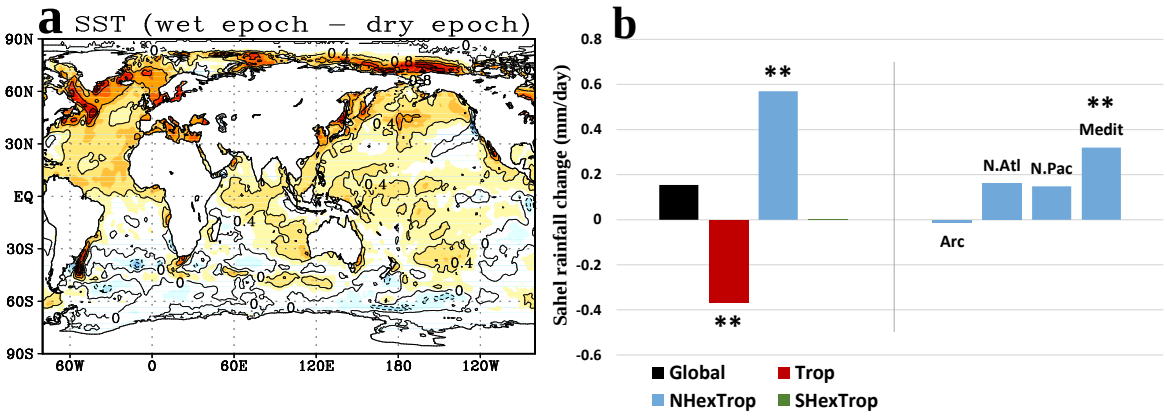

Figure 4.8. ***a****, The JAS-mean SST difference between earlier dry epoch (1970-1985) and later wet epoch (1994-2013).* ***b****, Simulated summer Sahel rainfall responses forced by global (black), tropical (red), NH extratropical (blue), and SH extratropical (green) SST anomalies in Fig.* ***a****. The NH extratropical impact is subdivided into four different NH extratropical ocean basins, Arctic, North Atlantic, North Pacific, and Mediterranean Sea. The significant rainfall responses are marked by single asterisk (*) indicating P < 0.10 and by double asterisks (**) indicating P < 0.05.*

A set of two experiments, in which the models are driven by historical global SSTs with and without historical variations in Mediterranean SSTs, clearly supports the critical role of Mediterranean warming in the recent Sahel rainfall recovery (cf. Figure 4.9a and b). The experiment shown in Figure 4.9a is similar to the AMIP experiment but forced only by historical global SST variations with fixed greenhouse gas concentrations. The SST forcing for the experiment shown in Figure 4.9b is the same as in Figure 4.9a, but with the fixed climatological monthly mean of Mediterranean SST. Thus, the impact of historical Mediterranean SST variation is not included in the latter experiment. The rainfall simulated by two AMIP-type experiments shows that the decreasing trends before the 1980s are reproduced well regardless of the presence of Mediterranean information, but there is a substantial difference in the rainfall trend after the 1980s. That is, the run with Mediterranean SST variation shows a positive rainfall trend in recent years (0.12mm day^{-1}/10yr), which is comparable to the recent observed rainfall recovery, while the other run produces a decreasing rainfall trend (-0.05mm day^{-1}/10yr). This implies that without the recent Mediterranean warming, the Sahel region might have experienced a continuous drying condition since the 1980s.

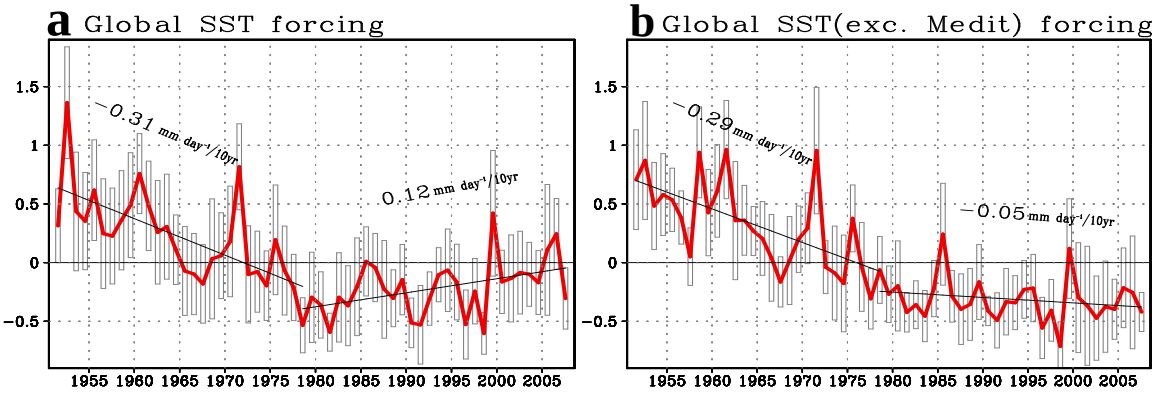

Figure 4.9. ***a****, Time series of JAS-mean Sahel rainfall simulated by ECHAM6 forced by historical AMIP2 SST forcing (1951~2007) with fixed greenhouse gas concentrations (CO2: 348ppm, CH4: 1620ppb, N2O: 312ppb). Bars represent +/− one standard deviations of 10 ensemble members and red line represents the ensemble mean. Rainfall trends in the earlier (1951-1978) and later periods (1978-2007) are shown with black lines.* ***b****, Same as* ***a****, except for the historical global SST forcing with fixed climatological monthly mean of Mediterranean SST. The trends for the later period (1978-2007) are significantly different between two experiments at* $P < 0.01$.

Although the future Mediterranean warming shown in Figure 3.8a is very likely due to the impact of increasing greenhouse gases, while the SST pattern associated with the recent Sahel rainfall increase shown in Figure 4.4b may not be simply attributed to the anthropogenic cause. To clarify that, we check whether the recent trends of Mediterranean warming simulated by various climate models are distinguished from their multi-century pre-industrial control (piControl) experiments. The multi-model data analysis shows that the trend of Mediterranean SST simulated by the control runs cannot exceed the magnitude of the recent warming trend (Figure 4.10). This indicates that the recent Mediterranean warming is most likely attributed to increasing anthropogenic greenhouse gases.

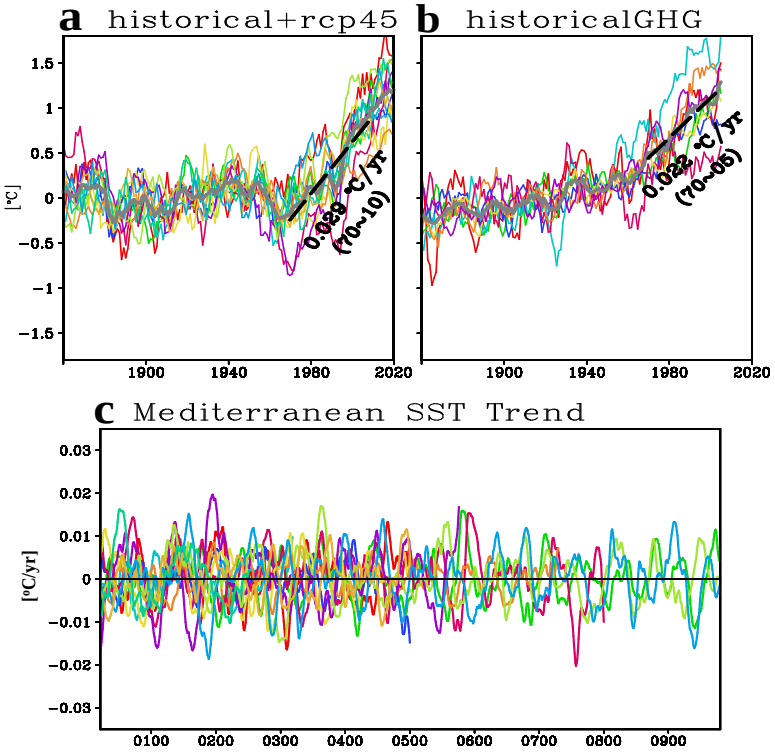

Figure 4.10. ***a****, The JAS-mean Mediterranean SST (0°-40°E; 30°-50°N) anomalies from historical and RCP4.5 (Representative Concentration Pathways 4.5) experiments simulated by 12 CMIP5 models. The thick grey line represents the ensemble mean SST anomalies, and the black dashed line shows the trend during the 40years form 1970 to 2010. The anomalies are the differences from the historical mean (1861-1970), and all the time series data are smoothed using a five-year running mean.* ***b****, Same as* ***a****, but from historical experiments forced by anthropogenic greenhouse gases only (historicalGHG). Note that the RCP4.5 starts from historical run, not from historicalGHG, thus the rainfall anomalies until 2005 are only plotted here.* ***c****, The 41-year sliding trends of Mediterranean SST from multi-century pre-industrial control (piControl) experiments simulated by different CMIP5 models.*

An interesting finding is that, compared to SST impact, the direct impact of greenhouse gases (not via SSTs) contributes negligible to the historical Sahel rainfall variations (cf. Figure 4.9a and Figure 4.11). This gives more credit to the mainstream view that historical SST forcing is dominant in driving the Sahel rainfall evolution (Folland et al. 1986; Bader and Latif 2003; Giannini et al. 2003; Rowell 2003; Lu and Delworth 2005; Martin and Thorncroft 2014), rather than to the view that the direct impact of greenhouse gases plays a dominant role in a warming climate (Dong and Sutton 2015). The minor portion of the direct greenhouse gas impact is consistent with our previous modelling result shown in Figure 2.10. One reason why in some models the direct impact of greenhouse gases predominates over the indirect impact via SST

could be their underperformance in simulating the historical SST-Sahel rainfall relationship, thereby muting the SST impact (Figure 4.12). Unlike many other CMIP5 models, HadGEM2 and CNRM-CM5 have a particularly weak sensitivity of Sahel rainfall responding to global SST variations. Overall results here suggest that, unlike the past Sahel rainfall variations, the recent Sahel wetting cannot be explained by tropical SST changes, but by the anthropogenic Mediterranean SST change that emerges as the key area of the recent Sahel rainfall change.

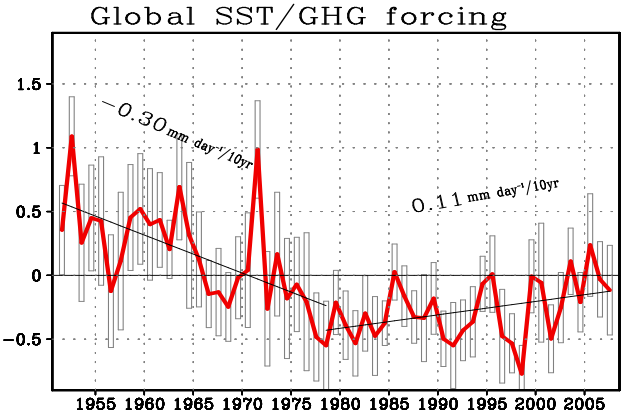

Figure 4.11. Time series of JAS-mean Sahel rainfall forced by historical AMIP2 SST forcing (1951~2007) and historical greenhouse gas forcing. Bars represent +/− one standard deviations of 10 ensemble members and red line represents the ensemble mean. Rainfall trends in the earlier (1951-1978) and later periods (1978-2007) are shown with black lines.

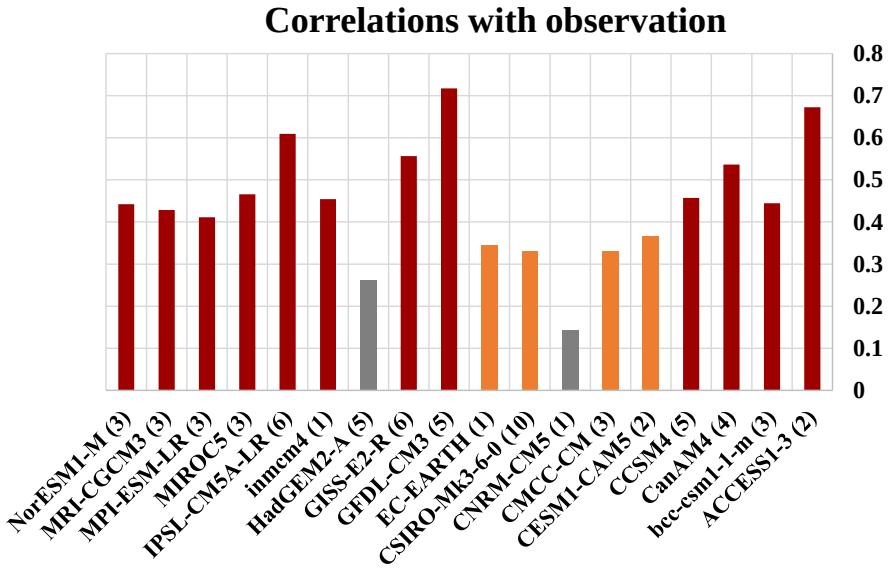

Figure 4.12. Correlation coefficients between simulated and observed Sahel rainfall. The JAS mean Sahel rainfall (10°W-30°E; 10°-20°N) during the period 1979-2008 is used both from

observation and models. The model data is obtained from AMIP simulations forced by historical SST. The numbers after individual model name refer to the number of ensemble members we used. The significant correlation coefficients are shaded by orange (P < 0.10) and red (P < 0.05) colors.

4.3 Mechanisms of Mediterranean - Sahel rainfall linkage

The mechanisms how the Mediterranean warming increases Sahel rainfall is consistent with previous works (Rowell 2003; Fontaine et al. 2010; Gaetani et al. 2010), showing that the more moist air by enhanced Mediterranean evaporation advects southward into the Sahel, and then leads to the enhanced low level moisture convergence and increased rainfall (Figure 4.13a). The north-easterly moisture flux anomalies from the Mediterranean Sea are mostly pronounced in June and July and provide a favourable condition for the increase in Sahel rainfall. This initial rainfall increase can induce a secondary circulation response and then intensify the south-westerly moisture flux from the tropical Atlantic in August and September (Figure 4.13b).

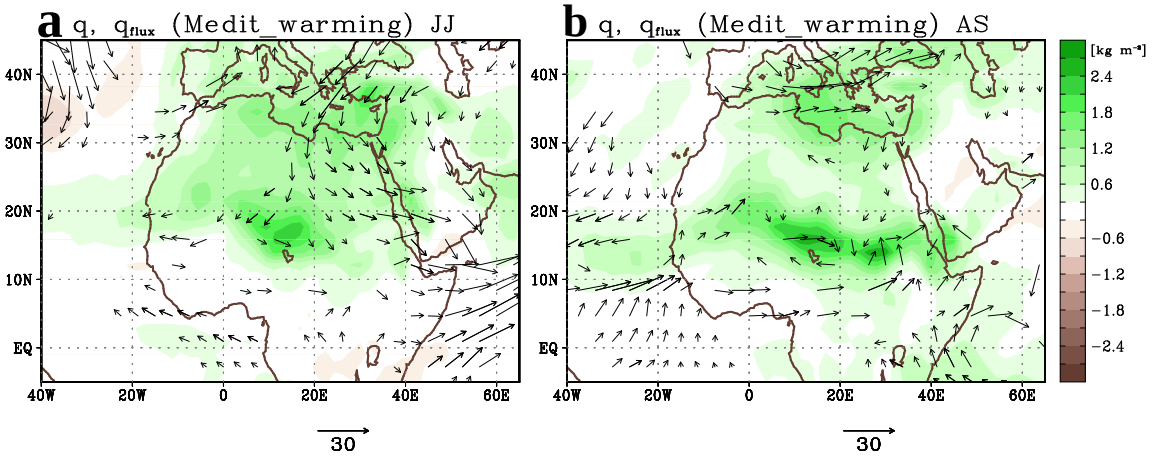

*Figure 4.13. The vertically-integrated moisture (shadings, unit: kg m^{-2}) and moisture flux (arrows, unit: kg m^{-2}·$m\ s^{-1}$) in (**a**) June-July and (**b**) August-September seasons simulated by the Mediterranean Sea warming experiment.*

A moisture budget analysis also demonstrates that the Sahel rainfall increase is dominated by the thermodynamic meridional moisture advection and convergence in

early monsoon season and then followed by the dynamic reinforcement of monsoon flow in late monsoon season (Figure 4.14). The precipitation minus evaporation (P - E) in the Mediterranean warming experiment is decomposed into a thermodynamic contributor related to moisture change with no circulation change, and a dynamic contributor related to circulation change with no moisture change. The thermodynamic component, particularly its meridional component, is the dominant factor in increasing rainfall in July, while the dynamic component becomes stronger and dominant in August and September. This wetting impact of both thermodynamic and dynamic effect may explain the emerging impact of the Mediterranean Sea in a warming climate. A possible reason why the wetting impact of the Mediterranean Sea is constantly increasing with the magnitude of SST warming is that unlike the tropical ocean warming which has a competition between the drying impact (by destabilizing troposphere) and the wetting impact (by increasing moisture), the Mediterranean warming can constantly increase the rainfall by both thermodynamic and dynamic enhancements without an opposing effect.

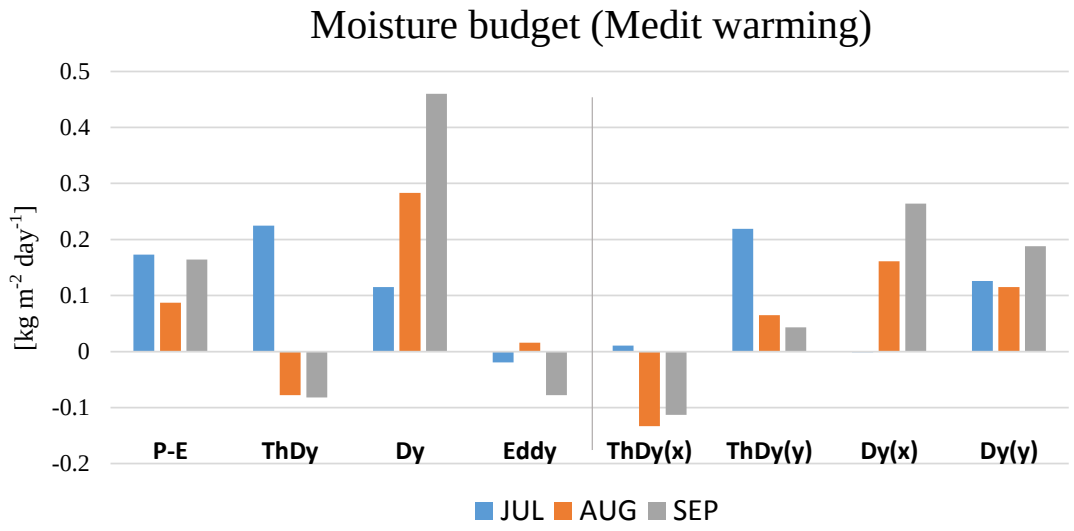

Figure 4.14. The difference of moisture budget between the Mediterranean warming experiment and control experiment (unit: kg m^{-2} day^{-1}). The 'P-E' refers to the difference between precipitation and evaporation changes, and the 'ThDy' and 'Dy' refer to the thermodynamic (involving moisture change, i.e. $-\int_0^{p_s} \nabla \cdot [\vec{\vec{U}}_{control}\, \delta\bar{q}]\, dp$) and dynamic (involving wind change, i.e. $-\int_0^{p_s} \nabla \cdot [\delta\vec{\vec{U}}\, \bar{q}_{control}]\, dp$) contributors to changes in 'P-E'. The 'Eddy' indicates the eddy contributor to 'P-E' changes. The 'ThDy(x)' and 'ThDy(y)' indicate the zonal and meridional component of thermodynamic contributor, respectively.

5 Local monsoon processes vs. global-scale ITCZ shift

The previous chapter has shown that the Mediterranean Sea warming is the critical pathway of the greenhouse gas impact on West African Monsoon rainfall in the recent past and the future. Given the strong NH extratropical warming found in the recent and future SST warming patterns that subsequently leads to an interhemispheric thermal contrast, it might be thought that the northward shift of tropical rain belt to balance the atmospheric energy transport is the main mechanism of the Sahel rainfall increase. However, the dominant impact of Mediterranean Sea warming compared to the impacts of warming in other NH extratropical ocean basins implies that the global-scale ITCZ shift may not be a key to understanding the Sahel rainfall increase. Rather, the local monsoon process related to the northerly moisture inflow seems to play a more important role. In this chapter, **the relative contribution of the local monsoon process versus global-scale ITCZ shift effect is examined** by performing a suite of aqua-planet experiments with an idealized land. The zonally uniform setting in this aqua-planet set-up allows to better interpret the global-scale Hadley cell change and assess its impact without the complexities introduced by Earth's land-sea distribution.[4]

[4] This chapter is based on the following manuscript: Park, J.-Y., J. Bader, and D. Matei, 2016: Local monsoon process vs. global-scale ITCZ shift: Which impact is more dominant for regional climate changes in a semi-arid tropical continent? *In preparation*.

5.1 Sahel rainfall and ITCZ shift mechanism

The historical Sahel rainfall variations are closely linked with global SST anomalies as described in Chapter 1 (Figure 1.6). An influential early study by Folland et al. (1986) showed that the persistent multiyear Sahel drought over the 20th century is associated with changes in the global SST pattern, which is characterized by an interhemispheric thermal gradient. Given that the global ITCZ generally shifts toward the warmer hemisphere and that the latitudinal location of ITCZ potentially affects Sahel rainfall, the underlying mechanism of the historical Sahel rainfall change often involves ITCZ shift dynamics caused by the thermal contrast between the hemispheres (Broccoli et al. 2006; Kang et al. 2008; Frierson et al. 2013). That is, if one hemisphere is warmer than the other, then a cross-equatorial Hadley circulation is induced to transport excessive energy to the colder hemisphere, and consequently pushing the tropical rain band toward the warmer hemisphere (Figure 5.1).

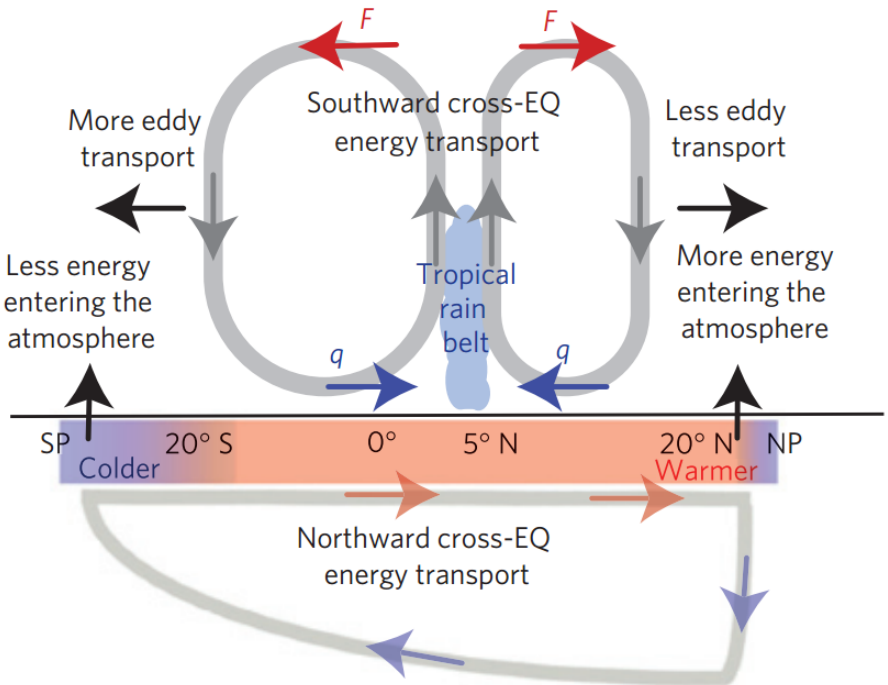

Figure 5.1. Schematic of the northward shift of ITCZ by NH extratropical warming from Frierson et al. (2013). The atmospheric energy imbalance between NH and SH extratropics caused by the oceanic meridional circulation shifts ITCZ toward the warmer hemisphere.

This ITCZ shift mechanism has been also highlighted by paleoclimate studies in linking millennial-scale variations of West African Monsoon to an interhemispheric temperature gradient. Paleoclimate proxy-data showed strong Sahel rainfall variability on longer timescales, such as the rainfall fluctuation in the last glacial maximum (approximately 23,000 ~ 18,000 years ago) or mid-Holocene (9000 ~ 6000 years ago) (Gasse 2000; Claußen et al. 2003). In the meanwhile, modelling studies on such paleoclimate periods have shown that a regional source of warming and cooling (e.g. changes in continental ice sheet or Atlantic meridional overturning circulation) can produce a hemisphere-wide temperature change, leading to an interhemispheric temperature gradient pattern (Manabe and Broccoli 1985; Broccoli 2000; AchutaRao and Sperber 2006). Gradually, the ITCZ shift mechanism by the interhemispheric thermal contrast has been adopted as a useful diagnostic in interpreting the paleo-hydroclimate changes in the Sahel.

With such a background, the present and future Sahel rainfall increase is assumed to be explained by the same ITCZ shift mechanism. It is because that the recent and future global warming patterns shown in previous chapters (Figure 3.8a and Figure 4.4b) are also characterized by hemispheric asymmetry patterns, thus the mechanism may be expected to hold for the present and future climate change. However, the impact of Mediterranean warming on Sahel rainfall is found to be dominant despite the existence of stronger warming in other extratropical ocean basins, implying that local moisture influx from the adjacent northern ocean is more important than the global-scale ITCZ shift mechanism. Hence, the relative importance of the moisture flux from the Mediterranean Sea (i.e. local monsoon process) and the northward shift of ITCZ (i.e. global-scale atmospheric energy transport) needs to be further assessed in explaining the relationship between Sahel rainfall increase and NH extratropical warming.

5.2 Aqua-planet experiments

5.2.1 Model set-up

The contribution of local monsoon impact to the present and future Sahel rainfall increase is examined through simplified model experiments on an aqua-planet set-up. The model used for this aqua-planet set-up is the ECHAM6, coupled to a slab ocean with zonal-mean ocean heat transport ('q-flux'). The q-flux, or so-called heat-flux correction of the slab ocean model, is derived from a 57-year-long AMIP simulation from 1951 to 2007 forced by the observed climatological mean sea surface temperature and sea ice concentration. The depth of slab ocean is set to 30-m and the sea ice formation is inhibited by permitting ocean temperatures to drop below the freezing temperature. Diurnal and seasonal cycles in insolation are included in the experiments, and a 360 days calendar is used. To avoid any explicit impact of stationary planetary waves on monsoon rainfall and difficulties in interpreting model responses, a zonally symmetric forcing is applied without considering aerosol and Halocarbons (CFCs), similar to those for the CMIP5 aqua-planet protocol. The prescribed greenhouse gases are set to as follows: CO_2:348 ppmv, CH_4:1650 ppbv, and N_2O:306 ppbv.

To disentangle the impact of local monsoon process from that of a global-scale ITCZ shift effect, we employed a reduction of evaporation over a certain ocean area. In the model, the turbulent moisture flux at the surface is given by

$$\mathrm{E} = \mathrm{C_q}\left|\overrightarrow{V_0}\right|(q_0 - q_{sfc})$$

where C_q is the moisture transfer coefficient over ocean, $\overrightarrow{V_0}$ is the horizontal wind velocity at the lowest level of the model, and q is specific humidity. The subscripts $_0$ and $_{sfc}$ represent values at the lowest level of the atmosphere and at the surface. Following Becker and Stevens (2014), the reduction of evaporation is achieved by rescaling the moisture transfer coefficient as follows.

$$\mathrm{C_q} \rightarrow \mathrm{C_q} \cdot \frac{1}{1+R}$$

Here, R is the evaporation resistance, which reduces evaporation with increasing R. In our experiment with a reduced evaporation set-up, R is set to 100, which is expected to reduce the evaporation coefficient by a factor of 101.

5.2.2 Experiments with an idealized continent

Three different simulations with the aqua-planet setup are conducted. In the control experiment, named as 'AquaLand', an Africa-like continent (15°W~45°E, 5°~30°N; 10°~45°E, 30°S~5°N) is introduced on the aqua-planet (Figure 5.2). The land surface properties over this idealized continent, such as surface albedo, orography, soil moisture, and vegetation type, are set to a uniformly fixed value for the simplicity of understanding underlying processes. In the second experiment, 5 Wm^2 of q-flux is imposed to the NH extratropical mixed layer ocean (north of 30°N), named as 'AquaLand_5W'. This run can be comparable to the NH extratropical warming experiment shown in the previous chapter. Finally, in the last experiment named as 'AquaLand_5W_R', the evaporation over the ocean (15°W~45°E, 30°~50°N) north of the idealized continent is reduced to see the impact of moisture influx from the adjacent northern ocean. The small area with the reduced evaporation is mimicking the Mediterranean Sea and designed to switch off the impact of local ventilation effect change by suppressing the increase in southward moisture flux under a NH extratropical warming condition. By doing so, the meridional moisture flux from the north in 'AquaLand_5W_R' is almost the same as that in the control run. The summary of experimental design is described in Table 5.1.

The purpose of this setup is to separate the impact of local monsoon process from that of ITCZ shift effect in present and future NH extratropical warming. The Sahel rainfall difference between extratropical warming run and control run, i.e. 'AquaLand_5W' and 'AquaLand', represents the impact of NH extratropical warming in which both local monsoon process and ITCZ shift dynamics involves. In 'AquaLand_5W_R', there is almost no increase in the moisture influx from the adjacent northern ocean compared to 'AquaLand', thus the rainfall difference between 'AquaLand_5W_R' and 'AquaLand' is expected to include the impact of ITCZ shift

dynamics only. Therefore, by comparing the results from these experiments, the role of local monsoon process in increasing Sahel rainfall under present and future NH extratropical warming can be evaluated.

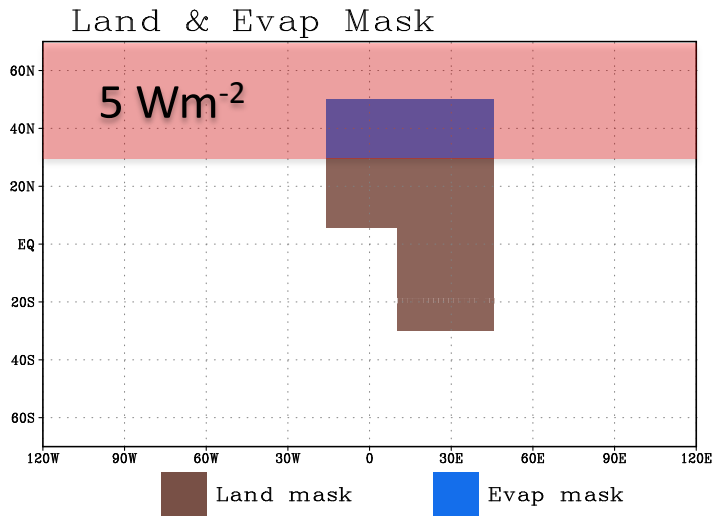

Figure 5.2. Land and evaporation mask for the idealized Africa-like land experiment. Brown shading represents the land area (15°W~45°E, 5°~30°N; 10°~45°E, 30°S~5°N) and blue represents the region where evaporation over the ocean is reduced (15°W~45°E, 30°~50°N). Red shading shows the area in which 5 W/m² of NH extratropical warming (0°~360°E, 30°~90°N) imposed.

Table 5.1 List of aqua-planet simulations with an idealized continent.

Run	Years	Specifications
AquaLand	50	Control run (includes 20 years of spin up)
AquaLand_5W	40	NH extratropical warming run (starts from end of Control run)
AquaLand_5W_R	40	NH extratropical warming run with reduced evaporation (starts from end of Control run)

5.3 Monsoon over an idealized continent

Before investigating how much the local monsoon process accounts for the Sahel rainfall increase under NH extratropical warming, it is desirable to assess whether the

idealized set-up can reproduce some important features of West African Monsoon. The reasonable modelling of the monsoon rainfall and of the associated circulation pattern can provide a reliable assessment of the relative importance of the local monsoon process and ITCZ shift effect.

5.3.1 Control experiment

The simulated monsoon from the control run, 'AquaLand', generally shows similar characteristics of African monsoon, such as the prevailing north-easterlies in winter over the monsoon region, south-westerlies in summer, and the associated seasonal march of tropical rain band (cf. Figure 1.4 and Figure 5.3). In summer, the south-easterly cross-equatorial winds turn toward the north-east and provide moist air to the West African Monsoon region over the idealized continent. This south-westerly monsoon flow together with north-easterly flows over the north-west of the continent form a cyclonic flow, which is corresponding to the Saharan Heat Low over the West Africa. Similar to the observational behaviour of the Saharan Heat Low (Lavaysse et al. 2009), the cyclonic flow over the idealized Africa continent exhibits the seasonal maximum of its intensity in July-August, and slightly weakens in September.

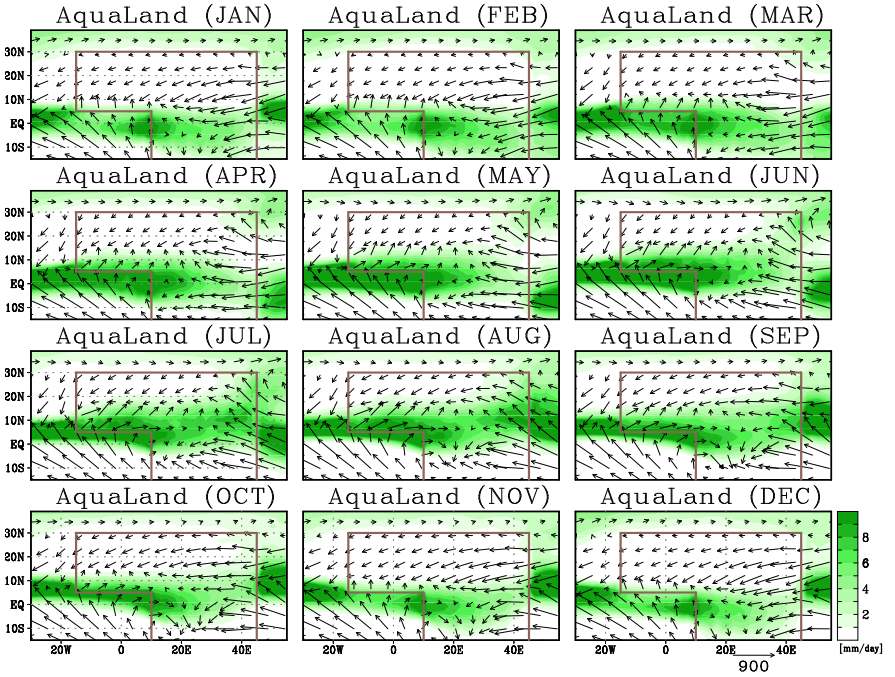

Figure 5.3. The climatological-mean rainfall (shading, unit: mm day^{-1}) and vertically-integrated low-level (1000-700hPa) moisture flux (arrows, unit: kg m^{-2}·m s^{-1}) from January to

December simulated by the control run, 'AquaLand'. Brown lines indicate the idealized land mimicking the African continent.

The vertical structure of the West African Monsoon system is quite distinctive from other monsoon systems and jets over the Sahel are known as important factors modifying the monsoon rainfall intensity. The zonal-mean vertical profile of wind and vertical motion simulated by the aqua-planet experiments show that the vertical structure of monsoon circulation also quite resembles that of the observations (Figure 5.4). The low-level African Westerly Jet at 900hPa and the mid-level African Easterly Jet at 600hPa are well represented in this idealized experiment despite the simplicity of the experimental set-up without any complex structure of the continent and heterogeneous land surface property. The shallow column of ascent produced by the low-level convergence of monsoonal winds and the deep core of ascent convection lying over the tropical rain band are also simulated reasonably well compared to the observation.

One caveat is that unlike the similar features in the low and mid-level circulation structures, the upper-level structure of zonal wind is quite different from the observation. The observed upper-level easterly jet at 200hPa, so-called Tropical Easterly Jet, is not present in the idealized run. It is because the Tropical Easterly Jet is generated by the north-south thermal contrast between the Indian continent and the Indian Ocean. Thus, the upper-level wind structure is not reproduced in the idealized set-up. The underestimation of the upper-level jet in the idealized run, however, implies that the upper-level circulation is not a major contributor to the monsoon system given the successful representation of West African Monsoon rainfall and the associated moisture convergence and upwelling. Overall results indicate that the idealized set-up can be used to test our hypothesis of local monsoon-driven Sahel rainfall increase under NH extratropical warming.

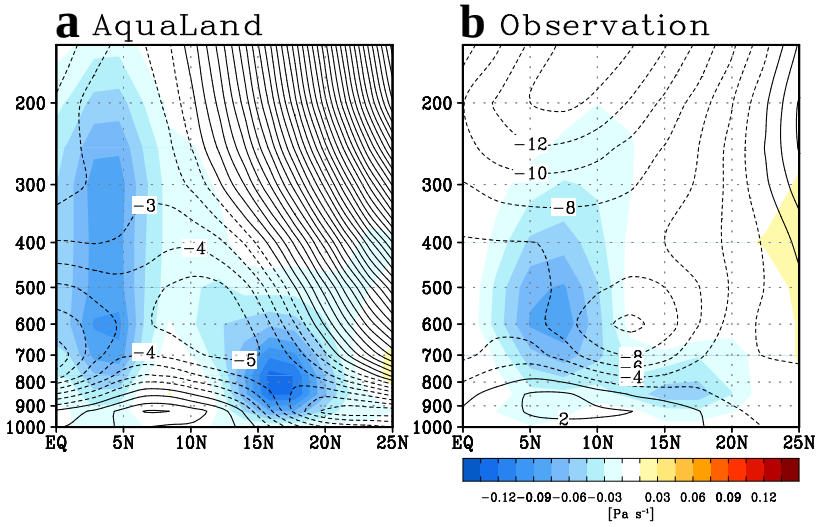

*Figure 5.4. The JAS-mean longitudinally-averaged (10°W-30°E) zonal wind (contour, unit: m/s) and vertical p-velocity (shading, unit: Pa/s) from (**a**) 'AquaLand' experiment and (**b**) observations. The observational data is obtained from NCEP2 reanalysis (Kanamitsu et al. 2002).*

5.3.2 NH extratropical warming experiment

It is also examined how NH extratropical warming affects the monsoon over the idealized continent. Similar to the NH extratropical warming case presented in previous chapters, the idealized experiment also shows that the extratropical warming leads to a northward expansion of summer rain band and an increase in monsoon rainfall (Figure 5.5 and Figure 5.6). The JAS-mean rainfall increases by about 40% in the extratropical warming case as will be quantified in Figure 5.8. The enhanced moisture convergence caused by the south-westerly and north-easterly monsoon flows and the seasonal evolution of the monsoon rainfall are also generally consistent to our previous results from more realistic experiments.

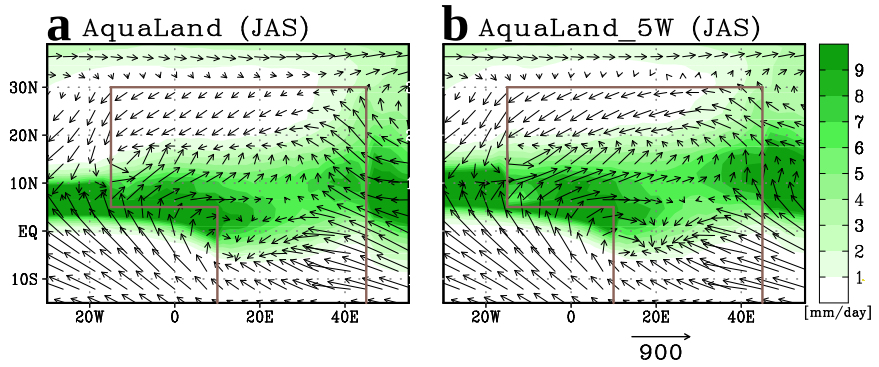

*Figure 5.5. The summer mean rainfall (shading, unit: mm day^{-1}) and vertically-integrated low-level (1000-700hPa) moisture flux (arrows, unit: kg m^{-2}·m s^{-1}) simulated by (**a**) control run, 'AquaLand', and (**b**) NH extratropical warming run, 'AquaLand_5W'. Brown lines indicate the idealized land.*

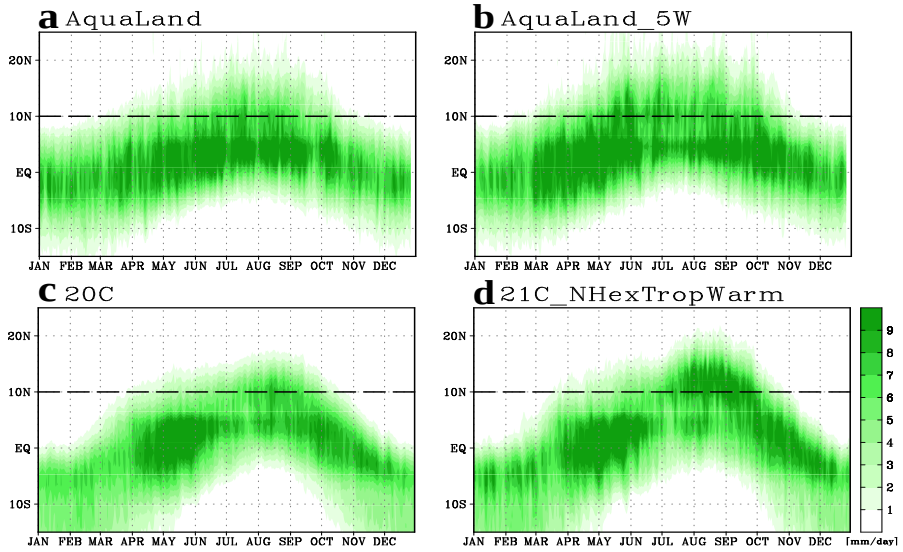

*Figure 5.6. Longitudinal precipitation mean over the idealized continent simulated from (**a**) 'AquaLand' and (**b**) 'AquaLand_5W' runs. **c** and **d** are same as **a** and **b** but for realistic AGCM experiments shown in Chapter 3, which are forced by 20th century SST and 21st century NH extratropical warming SST simulated by MIROC-ESM, respectively.*

One notable difference in the idealized warming case compared to the realistic experiment is that there is a strong inland penetration of tropical rain belt, extending further north above 20°N latitude (Figure 5.6b). This strong northward penetration is presumably due to the homogeneous setting of land surface albedo in the idealized experiment, which has a much lower surface albedo compared to high values over the Sahara. A supplementary experiment with the high surface albedo over the northern

Africa indeed demonstrates that the tropical rain belt cannot penetrate 20°N latitude even with the same magnitude of extratropical warming. Another reason could be the moisture influx from the eastern ocean that is generally not evident in observations due to the orographic barriers located in the eastern part of Africa. Despite such differences, the major characteristics of Sahel rainfall increase by extratropical warming are well reproduced in the idealized experiments. Thus, the mechanism of the NH extratropical warming impact on Sahel rainfall in this idealized experiment seems to be comparable to that seen in our previous realistic experiments, ensuring the validity of this simple setup to test our hypothesis.

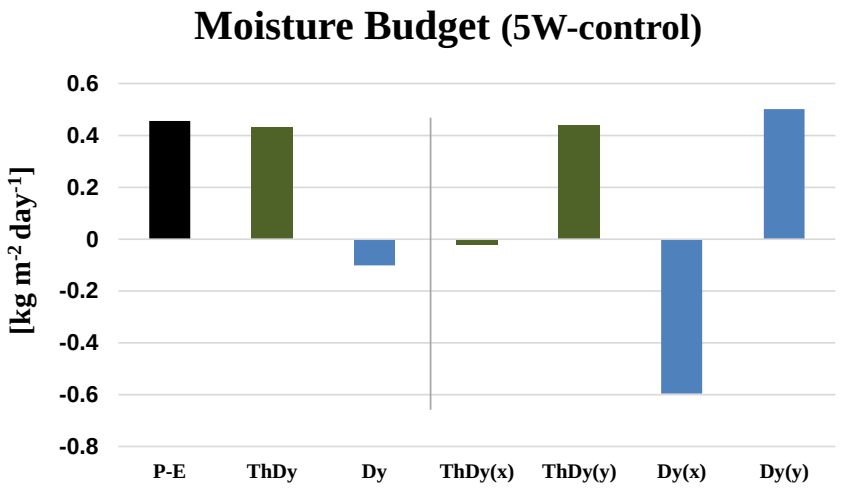

Figure 5.7. The difference of JAS mean moisture budget between 'AquaLand_5W' and 'AquaLand'. The 'P-E' refers to the difference between precipitation and evaporation changes, and the 'ThDy' and 'Dy' refer to the thermodynamic (involving moisture change, i.e. $-\int_0^{p_s} \nabla \cdot [\vec{\bar{U}}_{control}\, \delta\bar{q}]\, dp$ *) and dynamic (involving wind change, i.e.* $-\int_0^{p_s} \nabla \cdot [\delta\vec{\bar{U}}\, \bar{q}_{control}]\, dp$*) contributors to changes in 'P-E'. The 'ThDy(x)' and 'ThDy(y)' indicate the zonal and meridional component of thermodynamic contributor, respectively.*

A moisture budget analysis has been conducted to see the detailed mechanism how the NH extratropical warming increases the monsoon rainfall (Figure 5.7). The result shows that the monsoon rainfall increase is mostly affected by thermodynamic factors (i.e. involving moisture changes, $\delta\bar{q}$) rather than dynamic factors (i.e. involving wind changes, $\delta\vec{\bar{U}}$). Among the thermodynamic factors, the meridional thermodynamic moisture advection and convergence contribute the most to the rainfall increase, which is consistent with the previous experiments shown in Figure

4.14. This implies that moisture flux from the adjacent northern ocean, such as the Mediterranean Sea in reality, could be a key to understanding Sahel rainfall increase due to NH extratropical warming.

5.4 Dominant role of local ventilation effect

The current experimental set-up is designed to quantify the impact of local northerly moisture flux on the extratropical warming-driven monsoon rainfall increase. It is expected to achieve this goal by suppressing the evaporation increase over the northern ocean in the 'AquaLand_5W_R' run. That is, the local northerly moisture flux in 'AquaLand_5W_R' is almost the same as that in the control run, 'AquaLand'. The relative importance of the local ventilation effect and global-scale ITCZ shift effect can be investigated by analysing the 'AquaLand_5W_R' run and comparing it with the other two idealized runs.

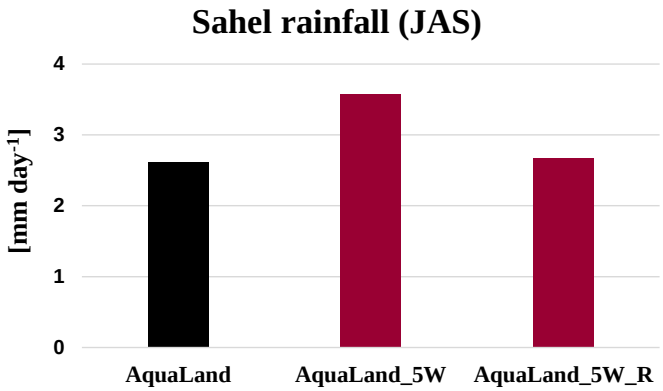

Figure 5.8. The JAS-mean Sahel rainfall (10°W-30°E; 10°-25°N) simulated from three different idealized experiments, AquaLand, AquaLand_5W, and AquaLand_5W_R.

The simulated summer rainfalls over the idealized Sahel area (10°W~30°E, 10°-25°N) are shown in Figure 5.8. The Sahel rainfall increases by about 40% in the extratropical warming case, 'AquaLand_5W'. A striking feature is that this Sahel rainfall increase almost disappears in 'AquaLand_5W_R' in which the NH extratropical warming still exists but the evaporation increase over the northern ocean is suppressed. Note that the summer mean northerly moisture fluxes (averaged over

the area between the Sahel and adjacent northern ocean, 10°W~30°E; 20°-30°N) simulated in 'AquaLand', 'AquaLand_5W', and 'AquaLand_5W_R' are 40.9, 49.4, and 41.9 kg m^{-2}·ms^{-1}, respectively, indicating a successful suppression of warming-induced moisture flux increase in 'AquaLand_5W_R'. The substantial decrease in Sahel rainfall in 'AquaLand_5W_R' compared to 'AquaLand_5W' supports our hypothesis that the key in the relationship between NH extratropical warming and Sahel rainfall increase is the local moisture supply from the adjacent northern ocean rather than the global-scale ITCZ shift effect. In other words, the NH extratropical warming cannot cause the significant increase in Sahel rainfall without additional moisture supply from the northern ocean, which corresponds to the Mediterranean Sea in the real world.

The circulation features associated with the decreased Sahel rainfall supports the weakened moisture supply from the north. The north-easterly moisture flux over the north of the continent is notably weaker in 'AquaLand_5W_R' than in 'AquaLand_5W' (Figure 5.9). This weakened moisture influx from the north is apparently due to the weaker evaporation over the northern ocean and consistent with the decreased rainfall. On the other hand, the south-westerly moisture flux is enhanced in 'AquaLand_5W_R' compared to 'AquaLand_5W'. The enhanced south-westerly monsoon flow generally provides more moisture to the Sahel region, thereby potentially increasing the monsoon rainfall. However, as seen in Figure 5.8, the monsoon rainfall actually decreases in 'AquaLand_5W_R', indicating that the drying impact of the weakened north-easterly flux plays a more dominant role than the wetting impact of the enhanced south-westerly moisture flux.

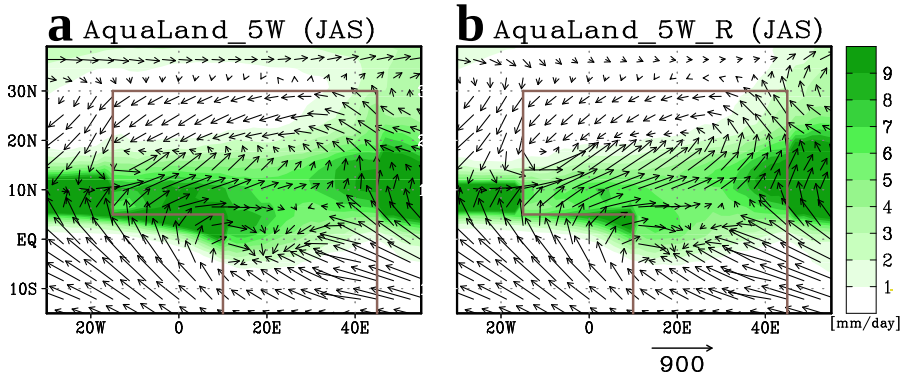

*Figure 5.9. Same as Figure 5.5 but for (**a**) 'AquaLand_5W' and (**b**) AquaLand_5W_R'.*

The enhanced south-westerly moisture flux in 'AquaLand_5W_R' is caused by the low pressure anomaly over the region where the warming-induced evaporation increase is suppressed (Figure 5.10). The weakened evaporation over the northern ocean reduces the latent heat release into the atmosphere, thus the ocean cannot efficiently release the energy enough to compensate the imposed 5 W/m^2 of warming. Consequently, the surface ocean temperature rises to release the excess energy through other surface layer fluxes, such as sensible heat and longwave radiation. This additional surface warming in the reduced evaporation region is a shortcoming of this experimental set-up, and it actually changes atmospheric circulations due to a low pressure anomaly over the northern ocean. This is why the south-westerly monsoon flow located at the southern flank of the low pressure anomaly is enhanced in 'AquaLand_5W_R'. However, given the less rainfall in 'AquaLand_5W_R' compared to 'AquaLand_5W', the wetting impact of this circulation change cannot explain the rainfall decrease. Rather, the weakened northerly moisture flux, presumably caused by the reduced evaporation and the subsequent moisture decrease, seems to overweigh the impact of the enhanced south-westerly moisture flux.

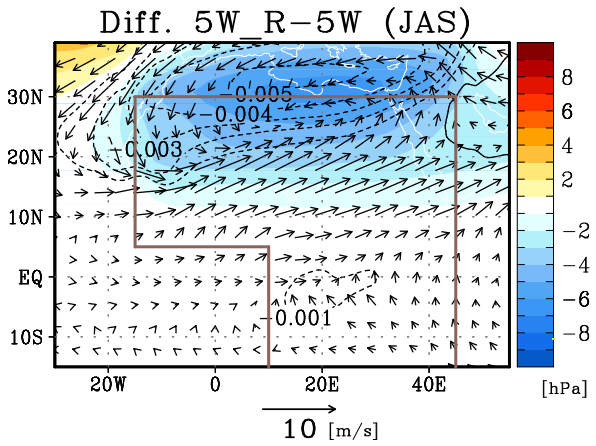

Figure 5.10. The JAS-mean difference in sea level pressure (shadings, unit: hPa), 925-hPa wind (arrows, unit: m/s), and 925-hPa specific humidity (contour, unit: g/g) between the two experiments, 'AquaLand_5W_R', and 'AquaLand_5W'.

The moisture budget analysis confirms that the substantial reduction of Sahel rainfall increase found in 'AquaLand_5W_R' is mostly related to the thermodynamic impact driven by the moisture decrease (Figure 5.11). The dynamical impact driven by

circulation changes appears to give a wetting impact on the Sahel rainfall. Here, the thermodynamic contributor to the decreased rainfall in 'AquaLand_5W_R' involves moisture change with no circulation change, while the dynamic contributor involves circulation change with no moisture change. Further decomposition of thermodynamic contributors into zonal and meridional components highlights that the meridional moisture advection and convergence involved with moisture changes are dominant thermodynamic contributors to the weaker monsoon rainfall in 'AquaLand_5W_R' than in 'AquaLand_5W'. The zonal component of thermodynamic contributor appears to have an opposite but weak effect. Consistent with the circulation change found in Figure 5.10, the dynamic contributor is dominated by the meridional component that includes meridional moisture advection and convergence associated with circulation change. This strong positive effect of the meridional component seems to be largely compensated by the negative effect of zonal component.

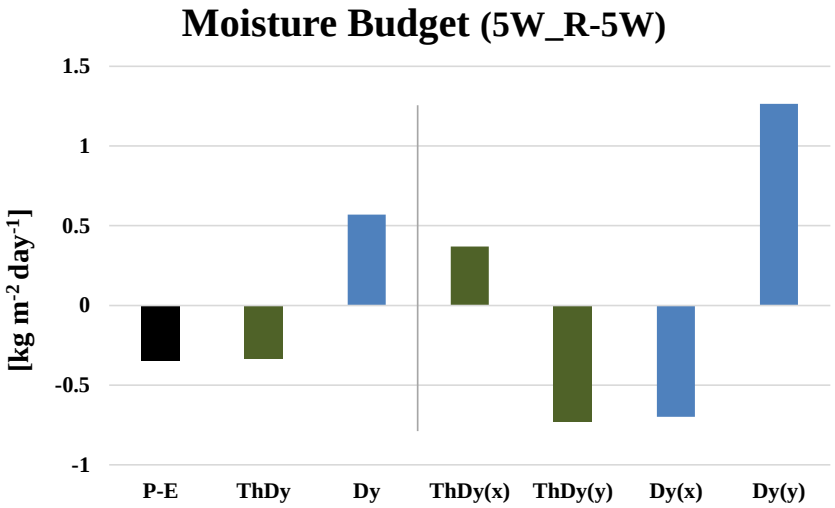

Figure 5.11. The difference of moisture budget between 'AquaLand_5W_R' and 'AquaLand_5W'. The 'P-E' refers to precipitation and evaporation changes, and the 'ThDy' and 'Dy' refer to the thermodynamic and dynamic contributors to changes in 'P-E'. The 'ThDy(x)' and 'ThDy(y)' indicate the zonal and meridional component of thermodynamic contributor, respectively.

The result from the moisture budget analysis is generally consistent with the previous result from comparing the NH extratropical warming run and control run,

'AquaLand_5W' and 'AquaLand'. That is, the thermodynamic impact of weakened moisture supply from the north plays a dominant role in the Sahel rainfall increase caused by NH extratropical warming. This suggests that, unlike a common belief, the global-scale ITCZ shift mechanism may contribute a minor effect to the Sahel rainfall increase although the NH extratropical warming causes an interhemispheric thermal gradient. In fact, the winter Hadley cell in 'AquaLand_5W_R' expands further north compared to the control run, which is the almost similar northward expansion as in 'AquaLand_5W' (Figure 5.12). The same feature can be found in the Hadley cell averaged over 10°W~30°E (Figure 5.13). If the ITCZ shift mechanism is the main driver of the Sahel rainfall increase under NH extratropical warming, then the similar northward shift of ITCZ in 'AquaLand_5W' and 'AquaLand_5W_R' would lead to a similar rainfall increase. However, as shown in Figure 5.8, the Sahel rainfall increase in 'AquaLand_5W' compared to the control run is substantially reduced in 'AquaLand_5W_R'. This implies that the reduced evaporation and the consecutive weakened moisture flux from the north is more important than the effect of northward shift of the ITCZ. We therefore conclude that, in contrast to oceanic ITCZ, the behaviour of the rain band over the African continent is not always dominated by the ITCZ shift effect driven by an interhemispheric thermal gradient, but the local ventilation effect of northerly monsoon flow may also play a dominant role.

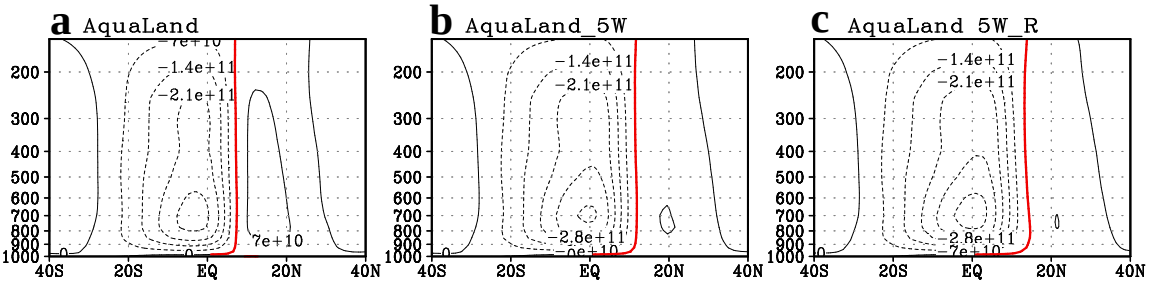

*Figure 5.12. The zonal-mean mass stream function averaged 0°-360°E from (**a**) AquaLand, (**b**) AquaLand_5W, and (**c**) AquaLand_5W_R. The red line indicates the zero line that refers to the location of ITCZ.*

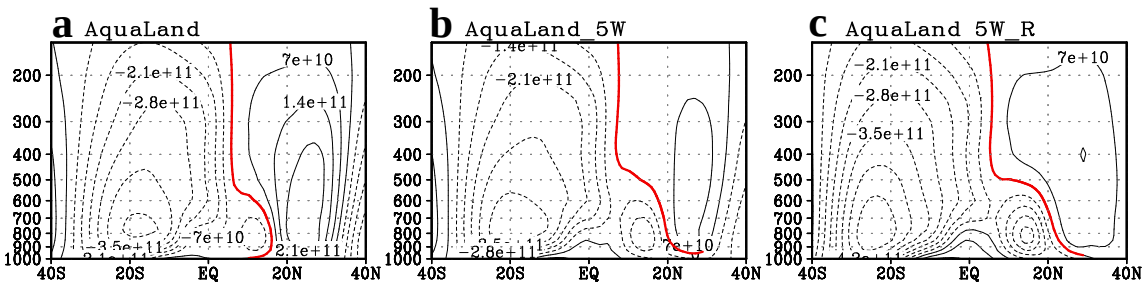

Figure 5.13. Same as Figure 5-12 but the zonal mean stream function averaged 10°W-30°E.

6 Conclusions

6.1 Summary and discussion

The aim of this thesis is to understand the disagreement in future West African Monsoon rainfall projected by current climate models and the underlying mechanisms of the future monsoon rainfall changes. By analysing a multi-model dataset and performing a series of idealized and realistic model experiments, this study provides an understanding of how the disparate Sahel rainfall projection arises. The addressed research questions and key findings are summarized as follows:

- **What is the source of the disparate future Sahel rainfall projections?**
  - The future NH extratropical warming relative to tropical warming is the key to the successful interpretation of the inter-model uncertainty in future Sahel rainfall.
  - In contrast to the past Sahel drought mainly caused by the tropical warming, the wetting impact of strong NH extratropical warming in the future can overweigh the drying impact of future tropical warming, suggesting a fundamental shift in the pathway of SST-Sahel rainfall relationship in a warming climate.

- **How does the NH differential warming affect future Sahel rainfall?**

- Tropical warming decreases Sahel rainfall due to the stabilized tropical atmosphere caused by strong upper-level warming and due to the insufficient increase in moist static energy over the convective margin.
- NH extratropical warming increases Sahel rainfall largely due to moisture supply from the Mediterranean Sea. The wetting impact of Mediterranean SST warming is proportionally increasing with the amplitude of SST warming, and emerging as a key to substantially control future Sahel rainfall by predominating over impacts of other NH ocean basins.
- The dominant impact of Mediterranean Sea in a warming climate is also found in the observed period, showing that the recent Sahel rainfall recovery cannot be explained without the recent Mediterranean Sea warming that is largely driven by anthropogenic forcing.
- The Sahel rainfall increase by Mediterranean warming is dominated by the thermodynamically-induced meridional moisture advection and moisture convergence in the early monsoon season and then followed by the dynamic reinforcement of monsoon flow in the late monsoon season.

- **Local monsoon process vs. ITCZ shift effect: Which process is more dominant for the Sahel rainfall increase by NH extratropical warming?**
  - Although the NH extratropical warming shifts the global ITCZ northward, it cannot cause the substantial increase in Sahel rainfall without additional moisture supply from the adjacent northern ocean, implying that ITCZ shift effect is not a dominant factor in this continental zone of ITCZ margin.
  - The enhanced northerly moisture flux and the subsequent rainfall increase are mostly related to the thermodynamic contributors involving moisture changes, which is consistent with our previous modelling results.

The dominant role of local monsoon processes in future Sahel rainfall, in particular involved with thermodynamic component of moisture changes, provides a new insight into understanding regional precipitation projections. It is challenging to build confidence in regional climate projections due to a number of difficulties, such as

systematic errors in models, sensitivity of regional climate to external forcing, and the relative role of internal variability. Previous works suggest that the thermodynamic component such as wet-get-wetter mechanism is well understood and most robust across the models. On the other hand, the dynamic component due to atmospheric circulation change has shown to be a major source of uncertainty in regional precipitation change (Xie et al. 2015). As shown in this study, however, the highly uncertain future Sahel rainfall is largely explained by the warming in the adjacent northern ocean (i.e. the Mediterranean Sea) and the subsequent thermodynamically-driven increase in northerly moisture flux. Thus, the thermodynamic component involving moisture changes cannot be ruled out as a main source of future rainfall uncertainty, particularly over continental tropical regions such as the Sahel. This suggests a distinctive characteristics of future rainfall change over this semi-arid region in Africa, which is different from the regional future rainfall change over the oceans. In this regard, understanding the mechanisms for NH extratropical warming, particularly warming in the adjacent ocean north of the continent and the corresponding moisture changes, is essential to reduce the future Sahel rainfall uncertainty and a key to more credible projections of future Sahel rainfall.

Over the past decade, the future projection of Sahel rainfall and the source of the discrepancies among the coupled GCMs have been issues of long-standing interest because of the historical climate-related calamities in this vulnerable area. This thesis demonstrates that the diverse magnitudes of NH extratropical warming simulated by the models, particularly those of Mediterranean Sea warming, are essential to understand the previously-reported conundrum of future Sahel rainfall behaviour. This finding establishes the small area, but potentially the most influential Mediterranean Sea as a key factor determining present and future Sahel rainfall trends. Looking ahead into the long-term future, greenhouse gases will continue to rise, which is likely to increase the NH extratropical SSTs including the Mediterranean sector. This may provide a favourable condition of persistent Sahel wetting as observed in recent years, although the impact of other factors cannot be ruled out, such as future changes in land surface properties, aerosols, and internal climate variability. Therefore, a careful investigation of how the NH SSTs responds to greenhouse gas-induced

warming, particularly warming in the Mediterranean Sea, is of great importance to obtaining more reliable estimates of future Sahel rainfall.

6.2 Envisaged future works

While conducting the present research on future West African Monsoon, several scientific questions that might be of interest to investigate further have arisen. Some future research topics and possible refinements of the experiments are the following.

The cause of model discrepancy in projected NH extratropical warming

The present study found that various magnitudes of future NH extratropical warming projected by current climate models are essential to understand the highly uncertain future Sahel rainfall changes. This naturally raises a question about what causes such different projections of future extratropical warming. It has been known that the strong NH extratropical warming and the subsequent interhemispheric temperature asymmetry are caused by several factors, such as the hemispheric asymmetry in land distribution, Southern Ocean vertical mixing, and sulphate aerosols unevenly distributed in the NH. However, this may not be the case for future projections given the same protocol used to force different CMIP5 models. Therefore, the model discrepancy in the NH extratropical warming is more likely linked to other factors, such as different model sensitivities to external forcing and different internal climate variabilities in individual model. The distinct patterns of tropical Pacific warming (i.e. La Niña-like warming or El Niño-like future warming) in the two groups of CMIP5 models, which project wet and dry future Sahel, are also possibly related to the distinct NH extratropical warming, considering the tropical-extratropical interaction through atmospheric wave disturbance and its footprint on the extratropical oceans. A comparison between two different versions of GFDL models may provide a clue on this issue. As shown in Figure 2.2, the GFDL-ESM2M(G) and GFDL-CM3 are developed from the same modelling group, but they project quite different magnitudes of future NH extratropical warming, and consequently leading to opposite future rainfall trends.

Sensitivity test of the present findings by using other climate models

This study relies on one model. Although the statistical analyses based on observations and CMIP5 multi-model dataset support the modelling results, it would be still important to repeat the present study with other AGCMs given the possibly different model sensitivities of Sahel rainfall response to global SST variations (Figure 4.12) or to increased greenhouse gases. For example, if another model has a different sensitivity of Sahel rainfall response to different ocean basins, then the relative dominance of the impacts of those ocean basins could be modified. In addition, although the model we used here, ECHAM6, shows a relatively good performance in simulating the historical SST impact on Sahel rainfall, it has not been tested how reasonably the Sahel rainfall responses to increased CO_2 in this model. The same experiments at higher resolution or with different set-ups of land surface properties may also advance the findings presented here.

Further refinement of Aqua-planet experiments

The aqua-planet experiment with a reduced evaporation set-up has a caveat as addressed in the previous chapter. That is, the ocean area with reduced evaporation, which is located north of the Africa-like continent, is artificially warmed to compensate the excess energy caused by the suppressed latent heat release. Although the circulation change caused by the increased surface temperature does not affect our main conclusions, a further refinement of the experimental set-up is necessary to avoid a possible misinterpretation of model responses and to yield a more robust conclusion. One way to remove the caveat is to allow the latent heat to be increased in the extratropical warming run, but artificially keeping the evaporation constant at the value of the control run (although it is not physically consistent). Another way would be removing the additional heat by changing ocean q-flux to compensate the temperature increase due to the suppressed latent heat release.

Revisiting the role of tropical easterly jet in West African Monsoon rainfall

A recent revised picture of the West African Monsoon suggests that the upper-level tropical easterly jet is a prime factor in the strong convection and the monsoon rainfall over the Sahel (Nicholson 2009b), rather than the low-level moisture convergence. That is, the moisture available for convection in this monsoon region is strongly coupled to the upper-level divergence and the subsequent uplift, which are controlled by the strength of the upper-level jet. Given the latitudinal position of the monsoon rainfall located at the right exit region of the easterly jet, however, the revised picture of West African Monsoon does not match with the conventional jet theory indicating the upper-level divergence and uplift at the left exit region of a jet streak. Moreover, as shown in our idealized aqua-planet experiments, the monsoon rainfall and its seasonal characteristics are generally reproduced well even without the strong easterly jet in the upper-level (Figure 5.4). This implies that the role of the upper-level jet may not be a key factor in the West African Monsoon rainfall, but a minor factor in affecting the monsoon rainfall intensity. Therefore, the role of upper-level easterly jet is worth revisiting and needs to be explicitly investigated.

Bibliography

AchutaRao, K., and K. R. Sperber, 2006: ENSO simulation in coupled ocean-atmosphere models: are the current models better? *Clim. Dyn.*, **27,** 1-15.

AMCEN, 2002: *Africa environment outlook: past, present and future perspectives.* Vol. 1, United Nations Envir Programme.

Bader, J., and M. Latif, 2003: The impact of decadal-scale Indian Ocean sea surface temperature anomalies on Sahelian rainfall and the North Atlantic Oscillation. *Geophys. Res. Lett.*, **30,** 2169.

Bader, J., and M. Latif, 2011: The 1983 drought in the West Sahel: a case study. *Clim. Dyn.*, **36,** 463-472.

Barandiaran, D., and S.-Y. Wang, 2014: The missing teleconnection between the North Atlantic and the Sahel precipitation in CFSv2. *Atmospheric Science Letters*, **15,** 21-28.

Becker, T., and B. Stevens, 2014: Climate and climate sensitivity to changing CO2 on an idealized land planet. *Journal of Advances in Modeling Earth Systems*, **6,** 1205-1223.

Biasutti, M., and A. Giannini, 2006: Robust Sahel drying in response to late 20th century forcings. *Geophys. Res. Lett.*, **33,** L11706.

Biasutti, M., I. M. Held, A. H. Sobel, and A. Giannini, 2008: SST forcings and Sahel rainfall variability in simulations of the twentieth and twenty-first centuries. *J. Clim.*, **21,** 3471-3486.

Biasutti, M., A. H. Sobel, and S. J. Camargo, 2009: The Role of the Sahara Low in Summertime Sahel Rainfall Variability and Change in the CMIP3 Models. *J. Clim.*, **22,** 5755-5771.

Biasutti, M., 2013: Forced Sahel rainfall trends in the CMIP5 archive. *J. Geophys. Res.*, **118,** 1613-1623.

Booth, B. B. B., N. J. Dunstone, P. R. Halloran, T. Andrews, and N. Bellouin, 2012: Aerosols implicated as a prime driver of twentieth-century North Atlantic climate variability. *Nature*, **484,** 228-U110.

Broccoli, A. J., 2000: Tropical cooling at the last glacial maximum: An atmosphere-mixed layer ocean model simulation. *J. Clim.*, **13,** 951-976.

Broccoli, A. J., K. A. Dahl, and R. J. Stouffer, 2006: Response of the ITCZ to Northern Hemisphere cooling. *Geophys. Res. Lett.*, **33,** L01702.

Caminade, C., and L. Terray, 2010: Twentieth century Sahel rainfall variability as simulated by the ARPEGE AGCM, and future changes. *Clim. Dyn.*, **35,** 75-94.

CARE, 2015: Sahel Hunger Crisis, accessed 22 October 2015 <http://www.care.org/emergencies/sahel-hunger-crisis>.

Chiang, J. C. H., and A. R. Friedman, 2012: Extratropical Cooling, Interhemispheric Thermal Gradients, and Tropical Climate Change. *Annual Review of Earth and Planetary Sciences, Vol 40*, **40,** 383-412.

Chou, C., J. D. Neelin, and H. Su, 2001: Ocean-atmosphere-land feedbacks in an idealized monsoon. *Quart. JR Met. Soc.*, **127,** 1869-1891.

Chou, C., and J. D. Neelin, 2004: Mechanisms of global warming impacts on regional tropical precipitation. *J. Clim.*, **17,** 2688-2701.

Claußen, M., V. Brovkin, A. Ganopolski, C. Kubatzki, and V. Petoukhov, 2003: Climate change in northern Africa: The past is not the future. *Climatic Change*, **57,** 99-118.

Cook, K. H., and E. K. Vizy, 2006: Coupled model simulations of the west African monsoon system: Twentieth- and Twenty-First-century simulations. *J. Clim.*, **19,** 3681-3703.

Cook, K. H., 2008: Climate science: The mysteries of Sahel droughts. *Nat. Geosci.*, **1,** 647-648.

Dong, B., and R. Sutton, 2015: Dominant role of greenhouse-gas forcing in the recovery of Sahel rainfall. *Nature Climate Change*.

Douville, H., D. Salas-Melia, and S. Tyteca, 2006: On the tropical origin of uncertainties in the global land precipitation response to global warming. *Clim. Dyn.*, **26,** 367-385.

Dunne, J. P., and Coauthors, 2012: GFDL's ESM2 Global Coupled Climate-Carbon Earth System Models. Part I: Physical Formulation and Baseline Simulation Characteristics. *J. Clim.*, **25,** 6646-6665.

Folland, C. K., T. N. Palmer, and D. E. Parker, 1986: Sahel rainfall and worldwide sea temperatures, 1901-85. *Nature*, **320,** 602-607.

Fontaine, B., S. Trzaska, and S. Janicot, 1998: Evolution of the relationship between near global and Atlantic SST modes and the rainy season in west Africa: statistical analyses and sensitivity experiments. *Clim. Dyn.*, **14,** 353-368.

Fontaine, B., and Coauthors, 2010: Impacts of warm and cold situations in the Mediterranean basins on the West African monsoon: observed connection patterns (1979-2006) and climate simulations. *Clim. Dyn.*, **35,** 95-114.

Frierson, D. M. W., and Coauthors, 2013: Contribution of ocean overturning circulation to tropical rainfall peak in the Northern Hemisphere. *Nat. Geosci.*, **6,** 940-944.

Gaetani, M., B. Fontaine, P. Roucou, and M. Baldi, 2010: Influence of the Mediterranean Sea on the West African monsoon: Intraseasonal variability in numerical simulations. *J. Geophys. Res.*, **115**.

Gaetani, M., and E. Mohino, 2013: Decadal Prediction of the Sahelian Precipitation in CMIP5 Simulations. *J. Clim.*, **26,** 7708–7719.

Gasse, F., 2000: Hydrological changes in the African tropics since the Last Glacial Maximum. *Quaternary Science Reviews*, **19,** 189-211.

Giannini, A., R. Saravanan, and P. Chang, 2003: Oceanic forcing of Sahel rainfall on interannual to interdecadal time scales. *Science*, **302,** 1027-1030.

Giannini, A., 2010: Mechanisms of Climate Change in the Semiarid African Sahel: The Local View. *J. Clim.*, **23,** 743-756.

Giannini, A., S. Salack, T. Lodoun, A. Ali, A. T. Gaye, and O. Ndiaye, 2013: A unifying view of climate change in the Sahel linking intra-seasonal, interannual and longer time scales. *Environmental Research Letters*, **8,** 024010.

Grist, J. P., and S. E. Nicholson, 2001: A study of the dynamic factors influencing the rainfall variability in the West African Sahel. *J. Clim.*, **14,** 1337-1359.

Haarsma, R. J., F. M. Selten, S. L. Weber, and M. Kliphuis, 2005: Sahel rainfall variability and response to greenhouse warming. *Geophys. Res. Lett.*, **32,** L17702.

Hakkinen, S., and P. B. Rhines, 2004: Decline of subpolar North Atlantic circulation during the 1990s. *Science*, **304,** 555-559.

Hastenrath, S., 1990: Decadal-scale changes of the circulation in the tropical atlantic sector associated with Sahel drought. *Inter. J. Climatol.*, **10,** 459-472.

Held, I. M., T. L. Delworth, J. Lu, K. L. Findell, and T. R. Knutson, 2005: Simulation of Sahel drought in the 20th and 21st centuries. *Proceedings of the National Academy of Sciences of the United States of America*, **102,** 17891-17896.

Herceg, D., A. H. Sobel, and L. Sun, 2007: Regional modeling of decadal rainfall variability over the Sahel. *Clim. Dyn.*, **29,** 89-99.

Hoerling, M., J. Hurrell, J. Eischeid, and A. Phillips, 2006: Detection and attribution of twentieth-century northern and southern African rainfall change. *J. Clim.*, **19,** 3989-4008.

IPCC, 2013: Climate change 2013: The physical science basis: IPCC Working group I contribution to the fourth assessment report of the IPCC.

Janicot, S., V. Moron, and B. Fontaine, 1996: Sahel droughts and ENSO dynamics. *Geophys. Res. Lett.*, **23,** 515-518.

Joly, M., A. Voldoire, H. Douville, P. Terray, and J.-F. Royer, 2007: African monsoon teleconnections with tropical SSTs: validation and evolution in a set of IPCC4 simulations. *Clim. Dyn.*, **29,** 1-20.

Kanamitsu, M., W. Ebisuzaki, J. Woollen, S. K. Yang, J. J. Hnilo, M. Fiorino, and G. L. Potter, 2002: NCEP-DOE AMIP-II reanalysis (R-2). *Bul. Am. Meteorol. Soc.*, **83,** 1631-1643.

Kang, S. M., I. M. Held, D. M. W. Frierson, and M. Zhao, 2008: The response of the ITCZ to extratropical thermal forcing: Idealized slab-ocean experiments with a GCM. *J. Clim.*, **21,** 3521-3532.

Kang, S. M., I. M. Held, and S.-P. Xie, 2014: Contrasting the tropical responses to zonally asymmetric extratropical and tropical thermal forcing. *Clim. Dyn.*, **42,** 2033-2043.

Kaptué, A. T., L. Prihodko, and N. P. Hanan, 2015: On regreening and degradation in Sahelian watersheds. *Proceedings of the National Academy of Sciences*, 201509645.

Kwon, M., J. G. Jhun, and K. J. Ha, 2007: Decadal change in east Asian summer monsoon circulation in the mid-1990s. *Geophys. Res. Lett.*, **34**.

Lavaysse, C., C. Flamant, S. Janicot, D. J. Parker, J. P. Lafore, B. Sultan, and J. Pelon, 2009: Seasonal evolution of the West African heat low: a climatological perspective. *Clim. Dyn.*, **33,** 313-330.

Liu, Y., J. C. Chiang, C. Chou, and C. M. Patricola, 2014: Atmospheric teleconnection mechanisms of extratropical North Atlantic SST influence on Sahel rainfall. *Clim. Dyn.*, 1-15.

Lu, J., and T. L. Delworth, 2005: Oceanic forcing of the late 20th century Sahel drought. *Geophys. Res. Lett.*, **32**.

Manabe, S., and A. J. Broccoli, 1985: The influence of continental ice sheets on the climate of an ice age. *J. Geophys. Res.*, **90,** 2167-2190.

Martin, E. R., C. Thorncroft, and B. B. B. Booth, 2014: The Multidecadal Atlantic SST-Sahel Rainfall Teleconnection in CMIP5 Simulations. *J. Clim.*, **27,** 784-806.

Martin, E. R., and C. D. Thorncroft, 2014: The impact of the AMO on the West African monsoon annual cycle. *Quart. JR Met. Soc.*, **140,** 31-46.

Mohino, E., S. Janicot, and J. Bader, 2011: Sahel rainfall and decadal to multi-decadal sea surface temperature variability. *Clim. Dyn.*, **37,** 419-440.

Neelin, J. D., C. Chou, and H. Su, 2003: Tropical drought regions in global warming and El Nino teleconnections. *Geophys. Res. Lett.*, **30,** 2275.

Nicholson, S. E., 2005: On the question of the "recovery" of the rains in the West African Sahel. *Journal of Arid Environments*, **63,** 615-641.

——, 2008: The intensity, location and structure of the tropical rainbelt over west Africa as factors in interannual variability. *Inter. J. Climatol.*, **28,** 1775-1785.

——, 2009a: On the factors modulating the intensity of the tropical rainbelt over West Africa. *Inter. J. Climatol.*, **29,** 673-689.

——, 2009b: A revised picture of the structure of the "monsoon" and land ITCZ over West Africa. *Clim. Dyn.*, **32,** 1155-1171.

Park, J.-Y., S.-W. Yeh, and J.-S. Kug, 2012: Revisited relationship between tropical and North Pacific sea surface temperature variations. *Geophys. Res. Lett.*, **39**.

Park, J.-Y., J. Bader, and D. Matei, 2014: Northern-hemispheric differential warming is the key to understanding the discrepancies in the projected Sahel rainfall. *Nature Communications*, **5,** 1-8.

Pattanaik, D. R., and V. Satyan, 2000: Fluctuations of Tropical Easterly Jet during contrasting monsoons over India: A GCM study. *Meteorology and Atmospheric Physics*, **75,** 51-60.

Ramage, C., 1971: Monsoon Meteorology. International Geophysical Series, Vol. 15. Academic Press.

Rotstayn, L. D., and U. Lohmann, 2002: Tropical rainfall trends and the indirect aerosol effect. *J. Clim.*, **15,** 2103-2116.

Rowell, D. P., 2003: The impact of Mediterranean SSTs on the Sahelian rainfall season. *J. Clim.*, **16,** 849-862.

Sobel, A. H., I. M. Held, and C. S. Bretherton, 2002: The ENSO signal in tropical tropospheric temperature. *J. Clim.*, **15,** 2702-2706.

Sutton, R. T., and D. L. R. Hodson, 2007: Climate response to basin-scale warming and cooling of the North Atlantic Ocean. *J. Clim.*, **20,** 891-907.

Taylor, K. E., R. J. Stouffer, and G. A. Meehl, 2012: An overview of CMIP5 and the experiment design. *Bul. Am. Meteorol. Soc.*, **93,** 485-498.

Trenberth, K., and Coauthors, 2007: *Observations: surface and atmospheric climate change. In: Climate Change 2007: The Physical Science Basis. Contribution of Working Group I to the Fourth Assessment Report of the Intergovernmental Panel on Climate Change.* Cambridge University Press, 235-336 pp.

United_Nations, 2015: UN water scarcity, accessed 20 October 2015, <http://www.un.org/waterforlifedecade/scarcity.shtml>.

Vizy, E. K., and K. H. Cook, 2001: Mechanisms by which Gulf of Guinea and eastern North Atlantic sea surface temperature anomalies can influence African rainfall. *J. Clim.*, **14,** 795-821.

Ward, M. N., 1998: Diagnosis and short-lead time prediction of summer rainfall in tropical North Africa at interannual and multidecadal timescales. *J. Clim.*, **11,** 3167-3191.

Watanabe, S., and Coauthors, 2011: MIROC-ESM 2010: model description and basic results of CMIP5-20c3m experiments. *Geoscientific Model Development*, **4,** 845-872.

Xie, S.-P., and Coauthors, 2015: Towards predictive understanding of regional climate change. *Nature Climate Change*, **5,** 921–930.

Zeng, N., J. D. Neelin, K. M. Lau, and C. J. Tucker, 1999: Enhancement of interdecadal climate variability in the Sahel by vegetation interaction. *Science*, **286,** 1537-1540.

List of Tables

List of Figures

Acknowledgements

Foremost, I would like to express my sincere gratitude to my principal advisor, Dr. Jürgen Bader, for giving me the opportunity to accomplish this Ph.D. at the Max-Planck-Institut für Meteorologie, for his continuous help both in science and daily life since I arrived at Hamburg Airport in January 2013 when my Hamburg life just started, and for his patience with the 'sometimes' wayward Ph.D student. I am also sincerely grateful to my co-advisor, Dr. Daniela Matei, for her sincere support and encouragement during my Ph.D study, for her pleasant energy that made our discussions cheerful and fun, and for her Midas Touch on our papers and the recommendation letters. I could not have imagined having better advisors and mentors for my Ph.D study.

I would like to thank Professor Dr. Martin Claußen for his careful and insightful comments on the progress of my Ph.D study and for his constant understanding on the side of the students. My sincere thanks also goes to the members of IMPRS office, Dr. Antje Weitz, Cornelia Kampmann, and Wiebke Böhm, for their great supports during the last three years.

I would also like to thank my room 313 members, Thomas Keitzl and Astrid Eichhorn, for their presence itself. Without them, my Ph.D life would have been much tougher and much less enjoyable.

Lastly, but certainly not least, I would like to thank my family. I must acknowledge by saying this: 사랑하고 감사합니다.